



**QUEEN'S
UNIVERSITY
BELFAST**

Designing effective homogeneous catalysis for glycerol valorisation: selective synthesis of a value-added aldehyde from 1,3-propanediol via hydrogen transfer catalysed by a highly recyclable, fluorinated Cp*Ir(NHC) catalyst

Ma, Y., Wang, Y., Morgan, P. J., Jackson, R. E., Liu, X., Saunders, G., Lorenzini, F., & Marr, A. C. (2018). Designing effective homogeneous catalysis for glycerol valorisation: selective synthesis of a value-added aldehyde from 1,3-propanediol via hydrogen transfer catalysed by a highly recyclable, fluorinated Cp*Ir(NHC) catalyst. *Catalysis Today*, 307, 248-259. <https://doi.org/10.1016/j.cattod.2017.09.036>

Published in:
Catalysis Today

Document Version:
Peer reviewed version

Queen's University Belfast - Research Portal:
[Link to publication record in Queen's University Belfast Research Portal](#)

Publisher rights

Copyright 2017 Elsevier.

This manuscript is distributed under a Creative Commons Attribution-NonCommercial-NoDerivs License (<https://creativecommons.org/licenses/by-nc-nd/4.0/>), which permits distribution and reproduction for non-commercial purposes, provided the author and source are cited.

General rights

Copyright for the publications made accessible via the Queen's University Belfast Research Portal is retained by the author(s) and / or other copyright owners and it is a condition of accessing these publications that users recognise and abide by the legal requirements associated with these rights.

Take down policy

The Research Portal is Queen's institutional repository that provides access to Queen's research output. Every effort has been made to ensure that content in the Research Portal does not infringe any person's rights, or applicable UK laws. If you discover content in the Research Portal that you believe breaches copyright or violates any law, please contact openaccess@qub.ac.uk.

Open Access

This research has been made openly available by Queen's academics and its Open Research team. We would love to hear how access to this research benefits you. – Share your feedback with us: <http://go.qub.ac.uk/oa-feedback>

Designing effective homogeneous catalysis for glycerol valorisation: selective synthesis of a value-added aldehyde from 1,3-propanediol *via* hydrogen transfer catalysed by a highly recyclable, fluorinated Cp*Ir(NHC) catalyst.

Yueyuan Ma,^a Yue-Ming Wang,^{a,b} Patrick J. Morgan,^a Rachael E. Jackson,^a Xiao-han Liu,^{a,b} Graham C. Saunders,^c Fabio Lorenzini,^{*a} and Andrew C. Marr.^{*a,b}

^a School of Chemistry and Chemical Engineering, Queen's University of Belfast, UK.

^b Queen's University Ionic Liquids Laboratories (QUILL), UK.

^c School of Science, The University of Waikato, Hamilton 3240, New Zealand.

**Fabio.Lorenzini@qub.ac.uk*

**a.marr@qub.ac.uk*

Abstract.

Hydrogen transfer initiated dehydration (HTID) of 1,3-propanediol (1,3-PDO), in ionic liquids, catalysed by a fluorinated Cp*IrCl₂(NHC) (Cp* = pentamethylcyclopentadienyl; NHC = carbene ligand) complex, allows selective production of propionaldehyde in high yields, under air. Isolation of the product is facilitated by the use of an ionic liquid as the solvent, enabling the reaction to be performed under reduced pressure. The Ir(III) catalyst in ionic liquid was proven to be highly recyclable. Removal of H and F atoms bound to the *ortho*-C atoms of the benzyl arm of the carbene ligand inhibits the catalytic activity of complexes Cp*IrCl₂(NHC), suggesting a crucial role played by the *ortho*-C-X grouping in HTID. The reaction of 1,3-PDO solutions in ionic liquid mimics that of the product of extraction of aqueous glycerol fermentation broths: the successful synthesis and isolation of a value-added chemical proves that valorisation of glycerol waste can be achieved. The combination of Cp*IrX₂(NHC) - catalysed HTID of 1,3-PDO in ionic liquids with bio-catalysis has then, ultimately, the potential to allow the transformation of waste glycerol into valuable chemicals that can be simply isolated.

Keywords: Iridium, catalysis, ionic liquids, glycerol, 1,3-propanediol, biomass.

Introduction.

For decades petrochemicals have been conveniently and economically generated concurrently with liquid fuel processing on a massive scale. As the human population increases, and the fossil fuel era dwindles, energy and chemicals technologies have to diversify. Many of the newer sources of useful energy cannot be coupled to chemicals production and new sources of chemicals are becoming important. Prior to the petrochemical era it was common to generate important bulk chemicals from biomass and this is again becoming profitable. Biomass is unique amongst the more renewable technologies as it can be employed to generate fuel and chemicals simultaneously in a biorefinery, this provides economics similar to petroleum and petrochemicals. Furthermore biomass is ubiquitous, as animals must eat. Ideally liquids fuels and chemicals will be derived from the waste from agriculture thus supporting, rather than competing with, food production. For example used vegetable oil can be transformed into biodiesel and the side product, glycerol, can be converted into chemicals.

In the biomass Renaissance one of the first platform chemicals to emerge was 1,3-propanediol. 1,3-propanediol (1,3-PDO) is a renewable platform chemical¹ that can be readily prepared by large scale whole cell biocatalysis.² Bio-derived 1,3-propanediol is currently produced by the bacterial fermentation of sugars, for example sugars derived from corn.^{2,3} 1,3-PDO can be obtained at a competitive cost and is commercially available from DuPont™ (marketed as Bio-PDO™).³ The whole cell biocatalytic preparation of 1,3-PDO introduced by DuPont™ and Tate & Lyle has considerable environment benefits compared to the petrochemical route.⁴ DuPont™ estimate a reduction in energy consumption of 40% and a reduction of greenhouse gas emissions of more than 40 %. Further improvements could be adopted by converting the feedstock to the by-product of biodiesel production, glycerol. 1,3-PDO is a major product of glycerol fermentation by *Clostridium*,⁵ *Klebsiella*, *Citrobacter*,⁶

1 U.S. Department of Energy (2004) Top Value Added Chemicals from Biomass (Vol. 1) (Ed's T. Werpy and G. Petersen), Pacific Northwest National Laboratory (PNNL), National Renewable Energy Laboratory (NREL), Office of Biomass Program (EERE). <http://www.eere.energy.gov/>.

2 T. Banner, A. Fosmer, H. Jessen, E. Marasco, B. Rush, J. Veldhouse, M. De Souza, "Biocatalysis for Green Chemistry and Chemical Process Development," ed's J. Tao and R. Kazlauskas, Wiley, New Jersey (2011) 429.

3 C.E. Nakamura, A.A. Gatenby, A. Kuang-Hua Hsu, R.D. La Reau, S.L. Haynie, M. Diaz-Torres, D.E. Trimbur, G.M. Whited, V. Nagarajan, M.S. Payne, S.K. Picataggio, R.V. Nair, US6013494, Jan 11 2000, "Method for the production of 1,3-propanediol by recombinant microorganisms", A, E. I. Du Pont De Nemours And Company, Genencor International.

4 C.S. Lee, M.K. Aroua, W.M.A.W. Daud, P. Cognet, Y. Pérès-Lucchese, P.-L. Fabre, O. Reynes, L. Latapie, *Renew. Sust. Energ. Rev.* 42 (2015) 963.

5 P. Kubiak, K. Leja, K. Myszka, E. Celinska, M. Spychała, D. Szymanowska-Powalowska, K. Czaczyk, W. Grajek, *Process Biochem.* 47 (2012), 1308.

6 R.K. Saxena, P. Anand, S. Saran, J. Isar, *Biotechnol. Adv.* 27 (2009) 895.

Lactobacillus,⁷ and genetically modified microorganisms.⁸ *Clostridium butyricum* has been shown to convert crude glycerol from biodiesel production to 1,3-PDO,⁹ further studies focused on direct crude glycerol fermentations have recently been reported.¹⁰

The Bio-1,3-PDO generated by DuPont™ is predominantly used for polymer synthesis. The importance of this biorenewable platform chemical has inspired us to investigate catalytic transformation of 1,3-PDO into other useful chemicals. We have previously shown that the biocatalytic conversion of glycerol to 1,3-PDO can be coupled to hydrogen transfer catalysed amination by using an ionic liquid as the phase for chemocatalysis in order to prepare secondary amines.⁹ Combining bio- and chemo-catalysis in this way removes the need for intermediate separation as 1,3-PDO can be extracted *in situ* by the solvent for chemocatalysis.¹¹ Ionic liquids were subsequently proven to be excellent solvents for the amination reaction enabling the fine-tuning of the product obtained.¹² More unexpected was the observation that dehydration of the diol occurred simultaneously with amination, this observation was quite unique in the reactivity of aliphatic alcohols and was most likely due to the 1,3-diol configuration.¹³ Further investigations revealed that, in the absence of amine dehydration could be affected to yield propionaldehyde as the major product.¹⁴ This occurs due to dehydrogenation of 1,3-PDO, which yields an aldol that rapidly dehydrates to acrolein and is then hydrogenated to propionaldehyde. This is a Hydrogen Transfer Initiated Dehydration (HTID) reaction. The reaction was catalysed by a Cp*IrCl₂(NHC) (Cp* = pentamethylcyclopentadienyl; NHC = carbene ligand) catalyst. Cp*Ir(III) complexes have excellent hydrogen transfer and dehydrogenation activity coupled to high air and water stability and have been demonstrated for amination,¹⁵ Oppenauer-type oxidation,¹⁶ dehydrogenation,¹⁷ the Guerbet reaction,¹⁸ and dynamic kinetic resolution (DKR).¹⁹

7 M.A. Ricci, A. Russo, I. Pisano, L. Palmieri, M. de Angelis, G. Agrimi, *J. Microbiol. Biotechnol.* 25 (2015) 893.

8 C.E. Nakamura, G.M. Whited, *Curr. Opin. Biotech.* 14 (2003) 454.

9 S.F. Liu, M. Rebros, G. Stephens, A.C. Marr, *Chem. Commun.* (2009) 2308.

10 (a) E. Wilkens, A.K. Ringel, D. Hortig, T. Willke, K.-D. Vorlop, *Appl. Microbiol. Biotechnol.* 93 (2012) 1057; (b) D. Dietz, A.-P. Zeng, *Bioprocess Biosyst. Eng.* 37 (2014) 225; (c) R. Dobson, V. Gray, K. Rumbold, *J. Ind. Microbiol. Biotechnol.* 39 (2012) 217.

11 A.C. Marr, S.F. Liu, *Trends Biotech.* 29 (2011) 199.

12 S.D. Lacroix, A. Pennycook, S. Liu, T.T. Eisenhart, A.C. Marr, *Catal. Sci. Technol.* 2 (2012) 288.

13 A.C. Marr, *Catal. Sci. Technol.* 2 (2012) 279.

14 Y.-M. Wang, F. Lorenzini, M. Rebros, G.C. Saunders, A.C. Marr, *Green Chem.* 18 (2016) 1751.

15 (a) M. Pera-Titus, F. Shi, *ChemSusChem* 7 (2014) 720; (b) G. Guillena, D.J. Ramón, M. Yus, *Chem. Rev.* 110 (2010) 1611; (c) S. Bähn, S. Imm, L. Neubert, M. Zhang, H. Neumann, M. Beller, *ChemCatChem* 3 (2011) 1853.

16 F. Hanasaka, K. Fujita, R. Yamaguchi, *Organometallics* 23 (2004) 1490.

17 (a) G.E. Dobreiner, R.H. Crabtree, *Chem. Rev.* 110 (2010) 681; (b) C. Gunanathan, D. Milstein, *Science* 341 (2013) 1229712; (c) J. Wu, D. Talwar, S. Johnston, M. Yan, J.-L. Xiao, *Angew. Chem. Int. Ed.* 52 (2013) 6983.

An example of the use of IrCp* complexes as efficient dehydrogenation catalysts was recently reported by J. Xiao and co-workers. A cyclometalated [Cp*Ir^{III}]/imino complex (Imine = 4-methoxy-*N*-[1-(3-methoxy-phenyl)ethylidene]aniline) was found to be a versatile catalyst for the rare, homogeneous, catalytic dehydrogenation of various benzo-fused *N*-heterocycles such as tetrahydroquinolines, tetrahydroisoquinolines, 3,4-dihydroisoquinolines, tetrahydro- β -carbolines, indolines, and tetrahydroquinoxalines. High yields of quinolines, isoquinolines, β -carbolines, indoles, and quinoxalines, respectively, were obtained using the cyclometalated [Cp*Ir^{III}]/imino complex, in concentration 0.1 – 1 mol %, in refluxing 2,2,2-trifluoroethanol.²⁰ Furthermore, in the case of isoquinolines and 3,4-dihydroisoquinolines, the Cp*Ir^{III} complex was also found to be an efficient catalyst for the reverse process, that is hydrogenation to tetrahydroisoquinolines: ultimately, J. Xiao and co-workers designed an interchangeable catalytic network that links the three forms of isoquinoline by hydrogenation and dehydrogenation equilibria, using the Cp*Ir^{III} catalyst in 2,2,2-trifluoroethanol at the specific temperatures and catalyst loadings allowing the six different transformations to occur as required. The ability of the Cp*Ir^{III} complex to catalyse the dehydrogenation of 3,4-dihydroisoquinolines was applied in a three-step total synthesis of papaverine, an opium alkaloid antispasmodic drug, clinically used for vasospasm treatment, while the Cp*Ir^{III}-catalysed dehydrogenation of tetrahydro- β -carbolines found application in a two-step total synthesis of harmine, a β -carboline alkaloid with cytotoxic activities against a series of tumor cell lines.

In the IrCp*-catalysed Guerbet reaction, a sequence of dehydrogenation, self aldol condensation, dehydration, and hydrogenation allows the transformation of primary aliphatic alcohols to dimeric alcohols *via* formation of aldehydes. In 2006 Y. Ishii and co-workers reported an efficient IrCp*-catalyzed Guerbet reaction of several primary linear, and branched, alcohols to β -alkylated primary alcohols under mild conditions: up to almost quantitative yields of the latter were obtained in *p*-xylene, at 120 °C, in the presence of KOH or *t*-BuOH, and hydrogen acceptors such as 1,7-octadiene, cyclooctene and 1-octene.^{18c}

18 (a) M. Guerbet, C. R. Acad. Sci. 128 (1899) 1002; (b) M. Guerbet, C. R. Acad. Sci. 149 (1909) 129; (c) T. Matsu-ura, S. Sakaguchi, Y. Obora, Y. Ishii, J. Org. Chem. 71 (2006) 8306.

19 (a) A.C. Marr, C.L. Pollock, G.C. Saunders, Organometallics 26 (2007) 3283; (b) R. Corberán, E. Peris, Organometallics 27 (2008) 1954; (c) T. Jerphagnon, R. Haak, F. Berthiol, A.J.A. Gayet, V. Ritleng, A. Holuigue, N. Pannetier, M. Pfeffer, A. Voelklin, L. Lefort, G. Verzijl, C. Tarabiono, D.B. Janssen, A.J. Minnaard, B.L. Feringa, J.G. de Vries, Top. Catal. 53 (2010) 1002; (d) C.L. Pollock, K.J. Fox, S.D. Lacroix, J. McDonagh, P.C. Marr, A.M. Nethercott, A. Pennycook, S. Qian, L. Robinson, G.C. Saunders, A.C. Marr, Dalton Trans. 41 (2012) 13423; (e) J.G. de Vries, Top. Catal. 57 (2014) 1306.

20 J. Wu, D. Talwar, S. Johnston, M. Yan, J. Xiao, Angew. Chem. Int. Ed. 52 (2013) 6983.

The production of propionaldehyde directly from 1,3-PDO, using a heterogeneous copper catalyst at high temperature, was reported by S. Sato *et al.* in 2008. The vapour-phase dehydration of 1,3-PDO over Cu-Al₂O₃ at 250 °C afforded propionaldehyde with 66 % selectivity.²¹ The dehydration of the substrate proceeded at 100 % conversion to yield propionaldehyde together with propanoic acid, 2-ethyl-1,3-dioxane, and acetaldehyde as by-products. The major by-product, propanoic acid, formed with 18 % selectivity, is likely to result from the oxidation of propionaldehyde with water as oxidant. S. Sato and co-workers suggested that formation of propionaldehyde from 1,3-PDO occurs either *via* a dehydrogenation–dehydration–hydrogenation or a dehydration–dehydrogenation–hydrogenation sequence. In the former route, the substrate is first dehydrogenated to form 3-hydroxypropanal; dehydration of the latter yields 2-propenal, which is finally hydrogenated to propionaldehyde. Alternatively, initial dehydration involving one of the hydroxy groups of 1,3-PDO leads to 2-propen-1-ol, which is then converted into propionaldehyde *via* dehydrogenation–hydrogenation: 2-propen-1-ol is first dehydrogenated to 2-propenal, which is then hydrogenated to propionaldehyde. Comparison with 1,3-butandiol (1,3-BDO) dehydration reactions suggests dehydrogenation–dehydration–hydrogenation to be the most likely reaction pathway. S. Sato and co-workers proposed this sequence for the copper catalyzed dehydration of 1,3-BDO to butanone: the diol is first dehydrogenated to 4-hydroxy-2-butanone; dehydration of the latter, leading to methyl vinyl ketone, followed by hydrogenation, affords butanone.²²

The C4 diol 1,3-BDO has been investigated as a model molecule for the catalytic transformation of polyols, including 1,3-diols such as 1,3-PDO, to carbonylic compounds: the understanding of its metal catalysed dehydration reactivity towards carbonylic compounds offers meaningful insights for the comprehension of the hydrogen transfer initiated dehydration of 1,3-PDO towards aldehydes hereby discussed.

1,3-BDO can undergo dehydration, dehydrogenation, or tandem dehydrogenation-dehydration-hydrogenation reactions, also followed by C-C bond cleavage reactions, to yield a range of valuable products. The initial selective dehydrogenation of either the primary or the secondary hydroxy group of 1,3-BDO would generate aldol compounds, namely hydroxyaldehyde, 3-hydroxybutanal, or hydroxyketones, 4-hydroxy-2-butanone, respectively. The following dehydration-hydrogenation will deliver further valuable chemicals, namely, in the case of 4-hydroxy-2-butanone, the α,β -unsaturated methyl vinyl ketone and the saturated methyl ethyl ketone. Otherwise, a different network of chemicals would be produced if the

21 S. Sato, M. Akiyama, R. Takahashi, T. Hara, K. Inui, M. Yokota, *App. Catal.*, A 347 (2008) 186.

22 S. Sato, R. Takahashi, H. Fukuda, K. Inui, *J. Mol. Catal. A: Chem.* 272 (2007) 164.

initial step is, instead, dehydration of 1,3-BDO: after formation of the unsaturated alcohols 3-buten-2-ol or 2-buten-1-ol or 3-buten-1-ol, further hydrogenation or dehydration reactions would deliver saturated alcohols, namely 1- or 2- butanol, or olefins, namely butadiene. Direct dehydration of 1,3-BDO to methyl ethyl ketone should also be considered. A clear picture of 1,3-BDO dehydrogenation / dehydration / hydrogenation product distribution has been reported recently by Di Cosimo and co-workers studying the gas-phase reaction of 1,3-BDO in the presence of bifunctional metal/acid-base ZCuMgAl catalysts (Z = 0.3 - 61.2 wt. % Cu, Mg/Al = 1.5 molar ratio), obtained with Cu–Mg–Al mixed oxides,²³ or silica supported copper catalysts ZCuSiO₂ (Z = 1 - 25 wt. % Cu).²⁴ Dehydrogenation of the 1,3-BDO secondary hydroxy group, prevailing over that of the primary one, followed by dehydration and hydrogenation, leads to the β -hydroxy ketone 4-hydroxy-2-butanone, the α,β -unsaturated ketone methyl vinyl ketone and the saturated ketone methyl ethyl ketone, as the major products, obtained in different relative amounts depending on the reaction conditions.

3-hydroxybutanal, the hydroxyaldehyde generated by the initial 1,3-BDO dehydrogenation occurring at the primary, instead of secondary, hydroxy group was observed only in minor concentrations at any reaction conditions using both the ZCuSiO₂ and ZCuMgAl catalysts; instead 4-hydroxy-2-butanone was always one of the main reaction products. That does not, however, rule out the occurrence of dehydrogenation at the primary hydroxy group: while it is known that secondary alcohols are better hydrogen donors than primary alcohols, indicating that the main 1,3-BDO dehydrogenation route involves the secondary hydroxy group, it should be considered that formation of 3-hydroxybutanal in low concentration could be due to C-C bond cleavage reactions, such as retro-aldol reactions, yielding minor compounds, namely the detected ethanol and acetaldehyde; while the dehydration-hydrogenation pathway predominates over the C-C bond breaking route for transformation of 4-hydroxy-2-butanone, the dehydration-hydrogenation products formed from 3-hydroxybutanal were observed in negligible amounts compared to the decomposition products ethanol and acetaldehyde.

Dehydrogenation at the primary hydroxy group of 1,3-BDO to aldehyde has recently been studied by M. Tamura, K. Tomishige and co-workers when investigating the production of butanone from C4 diols in the presence of Rh-MoO_x / SiO₂ catalyst *via* an intramolecular borrowing hydrogen methodology combining dehydrogenation and hydrogenolysis.²⁵

23 P.A. Torresi, V.K. Díez, P.J. Luggren, J.I. Di Cosimo, Catal. Sci. Technol. 4 (2014) 3203.

24 P.A. Torresi, V.K. Díez, P.J. Luggren, J.I. Di Cosimo, App. Catal., A 458 (2013) 119.

25 M. Tamura, T. Arai, Y. Nakagawa, K. Tomishige, Chem. Lett. 46 (2017) 1333.

Dehydrogenation at the primary hydroxy group was reported as less favourable than that at the secondary hydroxy group, which yields ketones. Dehydration activity and selectivity towards butanone lowered when moving from 2,4- to 1,3-BDO: adsorption of the primary hydroxy groups of the latter on the MoO_x species, where dehydrogenation of hydroxy groups generally occurs, is more favoured than that of secondary hydroxy groups; therefore, aldehydes, instead of ketones, should be produced in the first instance. However, production of CO₂ and alkenes prove that the aldehydic group is indeed formed, but undergoes rhodium catalysed decarbonylation or decarboxylation, and / or retro-aldol condensation. As a consequence, dehydrogenation of the secondary OH group still allows formation of 2-butanone, but at lower activity and selectivity.

The evidence reported by Di Cosimo and co-workers, and M. Tamura, K. Tomishige and co-workers, on the reactivity of primary hydroxy groups of 1,3-BDO towards aldehydes, along with the absence of any competing secondary hydroxy group in 1,3-PDO, support the proposed occurrence of the 1,3-PDO dehydrogenation–dehydration–hydrogenation sequence in the herein reported HTID of 1,3-PDO, which contains only primary hydroxy groups, to deliver the target propionaldehyde.

The success of the methyl, benzyl NHC ligand in the Cp*IrCl₂(NHC) catalytic system in HTID¹⁴ inspired us to look at the effects of altering the ring substituents on the benzyl group. The efficient, selective production of propionaldehyde *via* HTID of 1,3-PDO, in ionic liquids, in the presence of a recyclable, fluorinated Cp*IrCl₂(NHC) catalyst precursor, is hereby presented.

Experimental.

1-Methylimidazole ($\geq 99\%$ w, Sigma-Aldrich), 2,4,6-trifluorobenzyl bromide (97% w, Fluorochem), 2,6-dimethylbenzyl bromide (97% w, Aldrich), 1,3-propanediol (98% w, Aldrich), K₂CO₃ (99.5% w, BDH), KOH (85% w, Riedel-de Haen), CsCO₃ (99.995% w, Sigma-Aldrich), propionaldehyde (97% w, Aldrich), 2-methyl-2-pentenal (97% w, Aldrich), 2-methyl-pentanal ($> 95.0\%$ w, TCI), propanol (97% w, Sigma-Aldrich), methanol ($\geq 99.9\%$ w, CHROMASOLV, for HPLC, Sigma-Aldrich), dichloromethane ($\geq 99\%$ w, for GC, Sigma-Aldrich), diethyl ether ($\geq 99.5\%$ w, for GC, Sigma-Aldrich), ethyl acetate ($\geq 99.8\%$ w, Lab-scan), pentane ($\geq 99.9\%$ w, CHROMASOLV, for HPLC, Sigma-Aldrich), chloroform ($\geq 99.8\%$ w, for GC, Sigma-Aldrich), CDCl₃ (99.8% w, Aldrich), decalite (speed plus, diatomaceous filter-aid, Acros Organics), were used as received. 1-ethyl-2,3-dimethyl-

imidazolium-*N,N*-bistriflimide (EmmimNTf₂)²⁶ and methyl-tri-*n*-octyl-ammonium-*N,N*-bistriflimide (N_{1,8,8,8}NTf₂)²⁷ were synthesized according to literature procedures. ¹H NMR spectra were run on 300 MHz and 400 MHz Bruker spectrophotometers. The chemical shifts are reported in ppm. Signal multiplicities are reported as singlet (s), doublet (d), triplet (t), and multiplet (m) (br = broad). GC/MS spectroscopic data were collected on a MassHunter Workstation Software – Qualitative Analysis – Version B.06.00 – Build 6.0.663.10 – Service Pack 1 – © Agilent Technologies, Inc. 2012. GC/MS column: Agilent Technologies, Inc.; 19091S-433UI; HP-5MS UI; 30 m X 0.250 mm; 0.25 Micron; –60 to 325/350C; SN: USE137316H. GC/MS spectroscopic data were processed on MassHunter Data Analysis – MassHunter GC/MS Acquisition B.07.01.1805 – 12-Mar-2014 – © 1989-2014 Agilent Technologies.

Synthesis of 3-methyl-1-(2,4,6-trifluorobenzyl)-imidazolium bromide (BzMIIm-3F).

1-methylimidazole (0.685 g, 8.3 mmol) was added to a dichloromethane (30.0 mL) solution of 2,4,6-trifluorobenzyl bromide (1.877 g, 8.3 mmol). The resulting, colourless solution was stirred for 48 hours. Solvent removal led to a colourless crystalline powder of **BzMIIm-3F** that was dried overnight (2.500 g; yield 98 %). **BzMIIm-3F** was recrystallised by diffusing diethyl ether (*ca.* 4.5 mL), or ethyl acetate (*ca.* 4.5 mL), or pentane (*ca.* 4.5 mL) into a chloroform (*ca.* 0.5 mL) solution of **BzMIIm-3F** (0.5 g, 1.7 mmol; or 0.25 g, 0.9 mmol; or 0.1 g, 0.4 mmol). ¹H NMR (CD₃OD, 400 MHz): δ_H 7.68 (d, *J*_{HH} = 1.9 Hz, 1 H, NCH=CHN), 7.66 (d, *J*_{HH} = 2.0 Hz, 1 H, NCH=CHN), 7.11 (dt, *J* = 7.9 Hz, *J* = 3.2 Hz, 2 H, C₆H₂F₃), 5.58 (s, 2 H, CH₂), 3.98 (s, 3 H, CH₃). ¹H NMR (CDCl₃, 400 MHz): δ_H 10.52 (s, 1 H, NCHN), 7.60 (br s, 1 H, NCH=CHN), 7.23 (br s, 1 H, NCH=CHN), 6.78 (m, 2 H, C₆H₂F₃), 5.65 (s, 2 H, CH₂), 4.15 (s, 3 H, CH₃). ¹³C{¹H} NMR (CD₃OD, 300 MHz): δ_C 166.89, 164.69, 164.54, 162.19, 162.04, 125.66 (C₆H₂F₃), 123.86, 108.19, 102.42 (CHNCH=CHN and CHNCH=CHN), 41.67 (CH₂), 36.91 (CH₃). ¹⁹F{¹H} NMR (CD₃OD, 400 MHz): δ_F – 105.69 (t, *J*_{FF} = 7.5 Hz, 1 F, *para*-F), – 112.90 (d, *J*_{FF} = 7.5 Hz, 2 F, *ortho*-F). Anal. calcd. for C₁₁H₁₀BrF₃N₂: C, 43.02; H, 3.28; N, 9.12. Found: C, 42.74; H, 3.42; N, 8.78. HRMS: Clcd. M⁺/Z = 227.08 ([M⁺]). Found: M⁺/Z = 227.0696 ([M⁺]).

26 J. Wei, T. Ma, X. Ma, W. Guan, Q. Liu, J. Yang, RSC Adv. 4 (2014) 30725.

27 J.M. Fraile, J.I. García, C.I. Herrerías, J.A. Mayoral, D. Carrié, M. Vaultier, Tetrahedron: Asymmetry 12 (2001) 1891.

Synthesis of η^5 -pentamethylcyclopentadienyl-iridium(3-methyl-1-(2,4,6-trifluorobenzyl)-imidazolin-2-ylidene)-dichloride (1-3F).

Ag₂O (0.075 g, 0.3 mmol) was added, in the absence of light, to a dichloromethane (30.0 mL) solution of **BzMIm-3F** (0.124 g, 0.4 mmol). The resulting mixture was stirred at room temperature for 1.5 hours. [Cp*IrCl₂]₂ (0.167 g, 0.2 mmol) was then added and the resulting mixture was stirred for 4 hours. The solution was then filtered through celite. Solvent removal led to the isolation of an orange crystalline powder of **1-3F**. Recrystallisation from CH₂Cl₂ and pentane led to the isolation of yellow crystals of **1-3F** (0.229 g; yield 87 %). ¹H NMR (CDCl₃, 400 MHz): δ_{H} 6.87 (d, $J_{\text{HH}} = 2.0$ Hz, 1 H, NCH=CHN), 6.76 (tm, $J = 8.0$ Hz, 2 H, C₆H₂F₃), 6.48 (d, $J_{\text{HH}} = 2.0$ Hz, 1 H, NCH=CHN), 5.96 (d, $J_{\text{HH}} = 15.0$ Hz, 1 H, CHH-C₆H₂F₃), 5.34 (d, $J_{\text{HH}} = 15.0$ Hz, 1 H, CHH-C₆H₂F₃), 4.00 (s, 3 H, NCH₃), 1.69 (s, 15 H, CCH₃). ¹³C{¹H} NMR (CDCl₃, 400 MHz): δ_{C} 156.92 (CHNCH=CHN), 122.92, 119.99 (CHNCH=CHN and CHNCH=CHN), 108.47, 108.24, 108.04, 101.21, 100.93, 100.65 (C₆H₂F₃), 88.99 (CCH₃), 43.15 (CH₂-C₆H₂F₃), 38.86 (NCH₃), 9.13 (CCH₃). ¹⁹F{¹H} NMR (CDCl₃, 400 MHz): δ_{F} -105.75 (t, $J_{\text{FF}} = 8.0$ Hz, 1 F, *para*-F), -109.87 (d, $J_{\text{FF}} = 8.0$ Hz, 2 F, *ortho*-F). Anal. calcd. for C₂₁H₂₄Cl₂F₃IrN₂: C, 40.39; H, 3.87; N, 4.49. Found: C, 39.61; H, 3.98; N, 4.26. HRMS: Clcd. M⁺/Z = 598.12 ([M-Cl]⁺). Found: M⁺/Z = 589.1185 ([M-Cl]⁺).

Synthesis of 3-methyl-1-(2,6-dimethyl)benzylimidazolium bromide (BzMIm-2CH₃).

1-methylimidazole (0.410 g, 5.0 mmol) was added to a dichloromethane (30.0 mL) solution of 2,6-dimethylbenzyl bromide (1.100 g, 5.5 mmol). The resulting solution was stirred for 48 hours. The solution, initially colourless, turned opaque during the course of the reaction. Solvent removal led to a colourless solid of **BzMIm-2CH₃** that was dried overnight (1.400 g; yield 99 %). **BzMIm-2CH₃** was recrystallised by diffusing diethyl ether (*ca.* 4.5 mL) into a dichloromethane (*ca.* 0.5 mL) solution of **BzMIm-2CH₃** (0.5 g, 1.7 mmol). ¹H NMR (CDCl₃, 400 MHz): δ_{H} 10.64 (s, 1 H, NCHN), 7.27 (br s, 1 H, NCH=CHN), 7.23 (br s, 1 H, NCH=CHN), 7.12 (m, 2 H, C₆(CH₃)₂H₃), 6.82 (br s, 1 H, C₆(CH₃)₂H₃), 5.62 (s, 2 H, CH₂), 4.13 (s, 3 H, NCH₃), 2.34 (s, 6 H, CCH₃). ¹³C{¹H} NMR (CDCl₃, 400 MHz): δ_{C} 138.49 (CHNCH=CHN), 131.05, 130.31, 130.20, 129.42 (C₆(CH₃)₂H₃), 123.06, 120.68 (CHNCH=CHN and CHNCH=CHN), 48.29 (CH₂), 37.13 (NCH₃), 20.12 (CCH₃). Anal. calcd. for C₁₃H₁₇BrN₂: C, 55.53; H, 6.09; N, 9.96. Found: C, 55.58; H, 5.56; N, 10.53. HRMS: Clcd. M⁺/Z = 201.14 ([M⁺]). Found: M⁺/Z = 201.1386 ([M⁺]).

Synthesis of η^5 -pentamethylcyclopentadienyl-iridium(3-methyl-1-(2,6-dimethyl)-imidazolin-2-ylidene)-dichloride (1-2CH₃).

Ag₂O (0.066 g, 0.3 mmol) was added, in the absence of light, to a dichloromethane (20.0 mL) solution of **BzMIm-2CH₃** (0.105 g, 0.4 mmol). The resulting mixture was stirred at room temperature for 1 hour. [Cp*IrCl₂]₂ (0.153 g, 0.2 mmol) was then added and the resulting mixture was stirred for 4 hours. The solution was then filtered through decalite, washing the residue with dichloromethane (2 x 20.0 mL). Solvent removal from the collected dichloromethane solution led to the isolation of an orange crystalline powder of crude **1-2CH₃**. Recrystallisation from CH₂Cl₂ (5.0 mL) and pentane (10.0 mL) led to the precipitation of an orange solid. After decanting the solvent, the solid was washed with pentane (3 x 20.0 mL), and then dried under vacuum, resulting in a pale orange powder of **1-2CH₃** (0.185 g; yield 76 %). ¹H NMR (CDCl₃, 400 MHz): δ_{H} 7.09 (d, 1 H, NCH=CHN), 7.07 (d, 1 H, NCH=CHN), 6.75 (m, 2 H, C₆(CH₃)₂H₃), 6.24 (t, 1 H, C₆(CH₃)₂H₃), 5.29 (d, 1 H, CHH), 4.73 (d, 1 H, CHH), 3.99 (s, 3 H, NCH₃), 2.30 (s, 6 H, CCH₃), 1.69 (s, 15 H, CCH₃). ¹³C{¹H} NMR (CDCl₃, 400 MHz): δ_{C} 155.33 (CHNCH=CHN), 131.57, 129.18, 128.89, 128.25, 125.04 (C₆(CH₃)₂H₃), 122.14, 120.21 (CHNCH=CHN and CHNCH=CHN), 88.80 (Cp*-CCH₃), 48.82 (CH₂), 39.01 (NCH₃), 20.45 (C₆(CH₃)₂H₃), 9.56 (Cp*-CCH₃). HRMS: Clcd. M⁺/Z = 568.22 ([M⁺]). Found: M⁺/Z = 568.2189 ([M⁺]).

Hydrogen transfer initiated dehydration (HTID) of 1,3-propanediol (1,3-PDO) in the presence of Cp*IrX₂(NHC) complexes.

HTID of 1,3-PDO in the presence of (A) 1-3F or (B) 1-2CH₃ and a base, in ionic liquid: screening reaction conditions.

1,3-PDO [see 1,3-PDO in (A) Table S1 or (B) Table S8], **1-3F** (see **1-3F** in Table S1) (A) or **1-2CH₃** (see **1-2CH₃** in Table S8) (B), a base (A: see Base in Table S1; B: see K₂CO₃ Table S8), and an ionic liquid (A: see Solvent in Table S1; B: see EmmimNTf₂ Table S8) were added to a 50 mL round bottom flask connected, through a distillation condenser, to a 50 mL glass tube. The mixture was reacted at the selected temperature (see T in (A) Table S1 or (B) Table S8), at a controlled pressure of *ca.* 0.350 bar, for six hours, stirring at 1000 rpm. The reaction product, a colourless liquid, was isolated by distillation, and was collected for the duration of the six hours reaction in the collecting glass tube kept at *ca.* -196 °C (N₂ (l) bath). After separation from the minor water layer (if collected), the crude product [see %

yield (based on **2**) in (A) Table S1 or (B) Table S8] was analysed by GC/MS [see (A) Table S11 or (B) Table S18] and ^1H NMR [see (A) Table S21 or (B) Table S28] spectroscopies. The reacted mixture, left in the 50 mL round bottom flask, was analysed by ^1H NMR spectroscopy.²⁸

Recycling experiments.

HTID of 1,3-PDO in the presence of 1-3F and K_2CO_3 , at 120 or 150 °C, in EmmimNTf₂, and at [1,3-PDO]:[Ir] \cong 75.0 or 220.0: 10 or 5 runs recycling experiments. (A: T = 150 °C, [1,3-PDO]:[Ir] \cong 75.0; B: T = 120 °C, [1,3-PDO]:[Ir] \cong 75.0; C: T = 150 °C, [1,3-PDO]:[Ir] \cong 220.0.)

1,3-PDO [see 1,3-PDO in entry 1 in (A) tables S2, S3 and S4, (B) tables S5 and S6, (C) table S7], **1-3F** [see **1-3F** in entry 1 in (A) tables S2, S3 and S4, (B) tables S5 and S6, (C) table S7], K_2CO_3 [see K_2CO_3 in entry 1 in (A) tables S2, S3 and S4, (B) tables S5 and S6, (C) table S7], and EmmimNTf₂ [see EmmimNTf₂ in entry 1 in (A) tables S2, S3 and S4, (B) tables S5 and S6, (C) table S7], were mixed in a 50 mL round bottom flask and reacted at (A, C) 150 °C or (B) 120 °C, using the same glassware apparatus, procedure and conditions as those described above for the screening reaction conditions experiments. The crude product [see % Yield (based on **2**) in entry 1 in (A) tables S2, S3 and S4, (B) tables S5 and S6, (C) table S7] was analysed by GC/MS [see entry 1 in (A) tables S12, S13 and S14, (B) tables S15 and S16, (C) Table S17] and ^1H NMR [see entry 1 in (A) tables S22, S23 and S24, (B) tables S25 and S26, (C) Table S27] spectroscopies. The reacted mixture, left in the 50 mL round bottom flask, was analysed by ^1H NMR spectroscopy. The following 9 or 4 (for the 10 and 5 runs recycling experiments, respectively) recycling experiments were carried out as follows: 1,3-PDO [see 1,3-PDO in (A) (10 runs recycling) entries 2-10 in tables S2 and S3, and (5 runs recycling) entries 2-5 in table S4, (B) (10 runs recycling) entries 2-10 in Table S5, and (5 runs recycling) entries 2-5 in Table S6, (C) (5 runs recycling) entries 2-5 in Table S7] and K_2CO_3 [see K_2CO_3 in (A) (10 runs recycling) entries 2-10 in tables S2 and S3, and (5 runs recycling) entries 2-5 in Table S4, (B) (10 runs recycling) entries 2-10 in Table S5, and (5 runs recycling) entries 2-5 in Table S6, (C) (5 runs recycling) entries 2-5 in Table S7] were added to the reacted mixture resulting from the previous recycling experiment, in the 50 mL

28 The successful isolation of highly pure **2** from the crude product *via* distillation at atmospheric pressure, at T \cong 43 °C, has been proven when testing the HTID of 1,3-PDO in the presence of **1-5H** (see Scheme 2). See Y.-M. Wang, F. Lorenzini, M. Rebros, G.C. Saunders, A.C. Marr, Green Chem. 18 (2016) 1751.

round bottom flask. The resulting mixture was reacted, and then analysed, as in the first cycle.

HTID of 1,3-PDO in the presence of 1-3F and K₂CO₃, and mercury, in EmmimNTf₂.

1,3-PDO (see 1,3-PDO in Table S9), **1-3F** (see **1-3F** in Table S9), K₂CO₃ (see K₂CO₃ in Table S9), mercury (three drops), and EmmimNTf₂ (see EmmimNTf₂ in Table S9) were mixed in a 50 mL round bottom flask and reacted at 150 °C, using the same glassware apparatus, procedure and conditions as those described above for the reactions in the absence of mercury. The crude product (see % yield (based on propionaldehyde (**2**) in Table S9) was analysed by GC/MS (Table S19) and ¹H NMR (Table S29) spectroscopies.

HTID of 1,3-PDO in the presence of 1-3F and K₂CO₃, and water, in EmmimNTf₂.

1,3-PDO (see 1,3-PDO in Table S10), **1-3F** (see **1-3F** in Table S10), K₂CO₃ (see K₂CO₃ in Table S10), water (3.0 mL), and EmmimNTf₂ (see EmmimNTf₂ in Table S10) were mixed in a 50 mL round bottom flask and reacted at 150 °C, using the same glassware apparatus, procedure and conditions as those described above for the reactions in the absence of water. The monophasic crude product was analysed by GC/MS (Table S20) and ¹H NMR (Table S30) spectroscopies.

Analysis of reaction product solutions of HTID of 1,3-PDO in the presence of 1-3F and a base, in ionic liquids: general methodology.

GC/MS spectroscopy allowed calculation of the amount of **5** in the isolated crude product solutions. The molar amount of **2**, **3** and **4**, relative to **5**, was then calculated *via* integration of the ¹H NMR spectrum of the isolated crude product solutions. Then, the amount of **2**, **3** and **4** in the isolated crude product solutions, and ultimately mass balance, was calculated by combining GC/MS and ¹H NMR spectroscopic information.

The GC/MS and ¹H NMR analyses of the reaction product solutions are hereby described.

GC/MS analysis of reaction product solutions.

- **CH₃CH₂CH₂OH / CDCl₃ / CH₃OH calibration.**

The substrate and internal standard CH₃OH solutions for calibration were prepared and then analysed by GC/MS spectroscopy according to the method that this group recently reported,¹⁴ leading to the following calibration curve:

$$y = 0.4449x - 0.0345 \quad (R^2 = 0.9938) \quad (x = C_5/C_6, y = A_5/A_6). \quad (\text{Eq. 1})$$

- **GC analysis of CH₃OH solutions of pure 2, 3, 4, and 5.**

Commercially available **2**, **3**, **4**, and **5** (*ca.* 0.005 g) were each dissolved in CH₃OH (1.0 mL). The resulting solutions were analysed by GC/MS spectroscopy. The resulting spectra¹⁴ were used as benchmarks in the GC/MS analysis of the reaction product solutions resulting from screening conditions experiments and catalyst recycling experiments.

- **General methodology for screening conditions and catalyst recycling experiments.**

A CH₃OH (1.0 mL) solution of a known amount of the reaction product solutions (**PS** in tables S11, S12, S13, S14, S15, S16, S17, S18, S19, S20) was prepared. The internal standard CDCl₃ (**6** in tables S11, S12, S13, S14, S15, S16, S17, S18, S19, S20) was added. The resulting solution was analysed by GC/MS spectroscopy. The areas of the peaks due to the substrate (A₅) and the internal standard (A₆) are reported, for each solution, in tables S11, S12, S13, S14, S15, S16, S17, S18, S19, S20. Equation Eq. 1 then allowed calculation of [**5**] (C₅). Entries 1-39 in Table S11, 1-10 in Table S12, 1-10 in Table S13, 1-5 in Table S14, 1-10 in Table S15, 1-5 in Table S16, 1-5 in Table S17, 1-2 in Table S18, entry 1 in Table S19 and entry 1 in Table S20 correspond to entries 1-39 in tables 1, S1, and S21, 1-10 in tables S2, S22, and S31, 1-10 in tables S3, S23, and S32, 1-5 in tables S4, S24, and S33, 1-10 in tables S5, S25, and S34, 1-5 in tables S6, S26, and S35, 1-5 in tables S7, S27, and S36, 1-2 in tables S8, S28, and 3, entry 1 in tables S9, S29, and 2, and entry 1 in tables S10, S30, and S37, respectively.

¹H NMR analysis of reaction product solutions: general procedure.

A CDCl₃ (*ca.* 0.7 mL) solution of the reaction product solutions (*ca.* 0.010 g) was prepared. The resonances due to the four main components **2**, **3**, **4**, and **5** (**2**, δ_H 9.78 (C(O)H, m, I₂ (tables S21, S22, S23, S24, S25, S26, S27, S28, S29, S30); **3**, δ_H 9.38 (C(O)H, s, I₃

(tables S21, S22, S23, S24, S25, S26, S27, S28, S29, S30)); **4**, δ_{H} 9.60 (C(O)H, d, $J_{\text{HH}} = 2.02$ Hz, I_4 (tables S21, S22, S23, S24, S25, S26, S27, S28, S29, S30)); **5**, δ_{H} 3.60 (CH₂OH, t, $J_{\text{HH}} = 6.64$ Hz, I_5 (tables S21, S22, S23, S24, S25, S26, S27, S28, S29, S30))) were investigated in the ¹H NMR spectrum of the resulting solutions. The normalised ratio of I_2 , I_3 , I_4 and I_5 allowed calculation of the molar ratio of **2**, **3**, **4**, and **5**, and ultimately the molar yield of **2**, **3**, **4**, and **5** (tables S21, S22, S23, S24, S25, S26, S27, S28, S29, S30), and the mass balance (MB) (tables S21, S22, S23, S24, S25, S26, S27, S28, S29, S30).

Results and discussion.

This group has recently reported the successful synthesis of propionaldehyde, in high yields and selectivities, *via* hydrogen transfer initiated dehydration (HTID) of 1,3-propanediol (1,3-PDO) in the presence of a Cp*IrCl₂(NHC) complex and a base, in ionic liquids as the solvent media.¹⁴ The HTID of 1,3-PDO in ionic liquids was found to be successful also in the presence of water, and air. Complex **1-5H** (Scheme 2) was found to be a highly recyclable catalyst precursor for the selective production of a range of C3 and C6 aldehydes. Highly pure propionaldehyde was successfully isolated under reduced pressure, and distillation, with production of minimal waste. The ionic liquid solutions of 1,3-PDO mimic the ionic liquid solutions produced by extraction of aqueous glycerol fermentation broths: the successful synthesis and isolation of a value-added chemical such as propionaldehyde from them represents the valorisation of waste to chemicals. The combination of Cp*IrX₂(NHC) catalysed HTID of 1,3-PDO in ionic liquids with bio-catalysis has then, ultimately, the potential to allow the transformation of waste glycerol into valuable chemicals that can be simply isolated.

The high activity, selectivity, and recyclability displayed by the catalyst precursor **1-5H** prompted us to investigate how the performance of Cp*IrX₂(NHC) complexes as catalyst precursors for HTID of 1,3-PDO could be maximised. The possible involvement of C-H activation occurring at the benzylic *ortho*-C in **1-5H**, and cyclometallation,²⁹ had to be considered, along with their possible, beneficial or detrimental, contribution to catalysis. Replacing then the C-H bond at the benzylic *ortho*-C in **1-5H** with the much stronger C-F bond³⁰ could have a significant effect on the catalytic activity of the Cp*IrX₂(NHC) complexes as catalyst precursors. Furthermore, replacing the C-H bond with a C-C bond would prevent *ortho*-C-X bond activation, and any orthometallation reactions.

29 (a) H.P. Thomas, Y.-M. Wang, F. Lorenzini, S.J. Coles, P.N. Horton, A.C. Marr, G.C. Saunders, *Organometallics* 36 (2017) 960; (b) M. Moselage, J. Li, L. Ackermann, *ACS Catal.* 6 (2016) 498; (c) P.B. Arockiam, C. Bruneau, P.H. Dixneuf, *Chem. Rev.* 112 (2012) 5879; (d) L. Keyes, A.D. Sun, J.A. Love, *Eur. J. Org. Chem.* (2011) 3985; (e) F. Lorenzini, P. Marcazzan, B.O. Patrick, B.R. James, *Can. J. Chem.* 86 (2008) 253; (f) M. Martín, E. Sola, S. Tejero, J.L. Andrés, L.A. Oro, *Chem. Eur. J.* 12 (2006) 4043; (g) X. Li, H. Sun, F. Yu, U. Flörke, H.-F. Klein, *Organometallics* 25 (2006) 4695; (h) E. Fernandez, A. Ruiz, C. Claver, S. Castillon, P.A. Chaloner, P.B. Hitchcock, *Inorg. Chem. Comm.* 2 (1999) 21; (i) O. López, M. Crespo, M. Font-Bardia, X. Solans, *Organometallics* 16 (1997) 1233; (j) S.D. Perera, B.L. Shaw, M. Thornton-Pett, *Inorg. Chim. Acta* 233 (1995) 103; (k) M. Crespo, M. Martinez, J. Sales, *Organometallics* 12 (1993) 4297; (l) C.M. Anderson, M. Crespo, G. Ferguson, A.J. Lough, R.J. Puddephat, *Organometallics* 11 (1992) 1177; (m) C.M. Anderson, R.J. Puddephat, G. Ferguson, A.J. Lough, *J. Chem. Soc., Chem. Comm.* (1989) 1297; (n) T.G. Richmond, C.E. Osterberg, A.M. Arif, *J. Am. Chem. Soc.* 109 (1987) 8091; (o) M.I. Bruce, R.C.F. Gardner, F.G.A. Stone, *J. Chem. Soc., Dalton Trans.* (1976) 81; (p) M.I. Bruce, B.L. Goodall, G.L. Sheppard, F.G.A. Stone, *J. Chem. Soc. Dalton Trans.* (1975) 591; (q) M.I. Bruce, R.C.F. Gardner, B.L. Goodall, F.G.A. Stone, R.J. Doedens, J.A. Moreland, *J. Chem. Soc., Chem. Comm.* (1974) 185.

30 (a) T. Zheng, J. Li, S. Zhang, B. Xue, H. Sun, X. Li, O. Fuhr, D. Fenske, *Organometallics* 35 (2016) 3538; (b) Y. Nakao, N. Kashihara, K.S. Kanyiva, T. Hiyama, *J. Am. Chem. Soc.* 130 (2008) 16170.

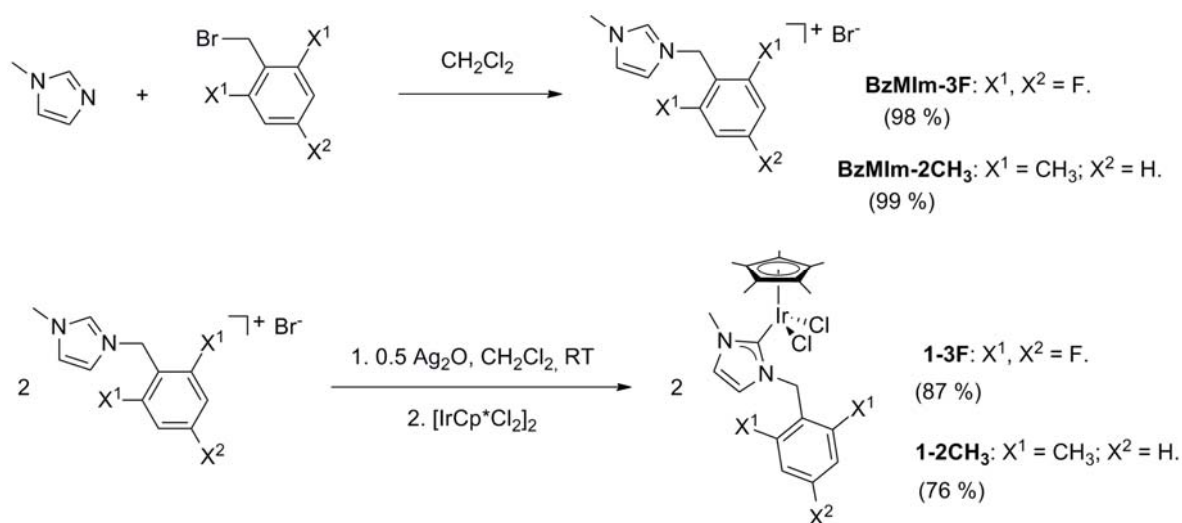
Synthesis of benzyl-imidazolium compounds **BzMIm-3F** and **BzMIm-2CH₃**, and of iridium complexes **1-3F** and **1-2CH₃**.

The complexes **1-3F** (see Scheme 1), in which both the benzylic *ortho*-C-H bonds have been replaced with a C-F bond (as well as the *para*-C-H bond), and **1-2CH₃** (see Scheme 1), in which both the *ortho*-C-H bonds have been replaced with two C-CH₃ bonds, were then synthesised, and their activity as catalyst precursors for HTID of 1,3-PDO in ionic liquids was tested. In addition, the substituents were chosen to have opposite effects on the overall electron density at the metal. The presence of three fluorine atoms on the benzyl arm of the carbene ligand bound to the metal centre in **1-3F** could allow a first test of how diminishing the electronic density on the metal centre would affect the catalytic activity of Cp*IrCl₂(NHC) complexes towards HTID of 1,3-PDO. Incorporating methyl functionality would increase the electron density.

Synthesis of **BzMIm-3F** and **BzMIm-2CH₃**.

Scheme 1 depicts the preparation of benzyl-imidazolium compounds **BzMIm-3F** and **BzMIm-2CH₃**, and then of the iridium complexes **1-3F** and **1-2CH₃**.

BzMIm-3F and **BzMIm-2CH₃** were synthesised following the synthetic procedure reported in the literature for analogous benzyl-imidazolium compounds.³¹ **BzMIm-3F** and **BzMIm-2CH₃** were isolated in excellent yields as air- and moisture-stable, crystalline solids after purification.



31 (a) Y. Gothe, T. Marzo, L. Messori, N. Metzler-Nolte, Chem. Eur. J. 22 (2016) 12487; (b) P.V. Simpson, K. Radacki, H Braunschweig, U. Schatzschneider, J. Organomet. Chem. 782 (2015) 116; (c) S. McGrandle, G.C. Saunders, J. Fluor. Chem. 126 (2005) 451.

Scheme 1. Synthesis of benzyl-imidazolium ligand precursors **BzMIm-3F** and **BzMIm-2CH₃**, and Cp*IrCl₂(NHC) complexes **1-3F** and **1-2CH₃**, via transmetalation of imidazolylidene ligands from silver carbene derivatives to [Cp*IrCl₂]₂.

BzMIm-3F was synthesised by reacting 1-methylimidazolium with (2,4,6-trifluoro)benzyl bromide in dichloromethane, under ambient pressure and at room temperature, for 24 hours.³¹ Highly pure **BzMIm-3F** was isolated in high yield (98 %) as a colourless crystalline solid (see Scheme 1). ¹H, ¹⁹F{¹H}, and ¹³C{¹H} NMR spectra of solutions of isolated **BzMIm-3F** show resonances typical of reported, analogous benzyl imidazolium compounds.³¹ The ¹H NMR spectrum of deuterated methanol solutions of isolated **BzMIm-3F** displays peaks that fall in the typical range for imidazolium C4 and C5 protons (δ_{H} 7.68, 7.66), benzylic protons (δ_{H} 5.58), *N*-methyl protons (δ_{H} 3.98), and aromatic protons (δ_{H} 7.11). The resonance due to the imidazolic C2 proton could only be detected in the deuterated chloroform solutions of **BzMIm-3F** (δ_{H} 10.52). The ¹⁹F{¹H} NMR spectrum shows the typical resonances due to the *para* fluorine atom and the two *ortho* fluorine atoms in the benzylic aromatic ring (δ_{F} -105.69 and -112.90, respectively). Peaks falling in the typical range for aromatic and imidazolic (δ_{C} 166.89-102.42), benzylic (δ_{C} 41.67), and *N*-methyl (δ_{C} 36.91) carbon atoms are observed in the ¹³C{¹H} NMR spectrum of deuterated methanol solutions of **BzMIm-3F**.

The method described for the synthesis of **BzMIm-3F** also allowed isolation of highly pure **BzMIm-2CH₃**, in high yield (99 %), as a colourless powder, from 1-methylimidazole and 2,6-dimethylbenzyl bromide (see Scheme 1). The resonances displayed in the ¹H NMR spectrum of deuterated chloroform solutions of isolated **BzMIm-2CH₃** fall in the typical range for imidazolic C2 protons (δ_{H} 10.64), imidazolium C4 and C5 protons (δ_{H} 7.27, 7.23), aromatic protons (δ_{H} 7.12, 6.82), benzylic protons (δ_{H} 5.62), and *N*- (δ_{H} 4.13) and *C*-methyl (δ_{H} 2.34) protons.³¹ The ¹³C{¹H} NMR spectrum exhibits peaks typical for aromatic and imidazolic (δ_{C} 138.49-120.68), benzylic (δ_{C} 48.29), and *N*- (δ_{C} 37.13) and *C*-methyl (δ_{C} 20.12) carbon atoms.³¹

Synthesis of 1-3F and 1-2CH₃.

1-3F and **1-2CH₃** were then synthesised, following the synthetic procedure reported in the literature for analogous Cp*IrCl₂(NHC) complexes, by transmetalation of 3-methyl-1-(2,4,6-trifluorobenzyl)-imidazolylidene and 3-methyl-1-(2,6-dimethyl)benzylimidazolylidene, respectively, from the corresponding silver carbene derivative to [Cp*IrCl₂]₂, in CH₂Cl₂ (see Scheme 1). The reactivity of Ag-NHC complexes towards NHC transfer has been reported for transmetalation reactions with Rh(I) and Ir(I)

complexes, and was also found to apply to $[\text{Cp}^*\text{IrCl}_2]_2$.^{31c,32} Compounds **1-3F** and **1-2CH₃** were isolated in good to excellent yields (87 and 76 %, respectively) as air- and moisture-stable, crystalline solids after purification.

The ^1H and $^{13}\text{C}\{^1\text{H}\}$ NMR spectra of the deuterated chloroform solutions of both **1-3F** and **1-2CH₃** display the expected resonances, falling at chemical shifts consistent with those reported in the literature for analogous $\text{Cp}^*\text{Ir}(\text{NHC})$ complexes.^{32,33}

No significant changes were observed regarding the chemical shift of the peaks corresponding to the aromatic and imidazolium methylic protons of **1-3F** as compared to the reacting ligand (aromatic: δ_{H} 6.76, vs. 6.78 in **BzMIm-3F**; NCH_3 : δ_{H} 4.00, vs. 4.15 in **BzMIm-3F**). The only resonance due to the two equivalent methylenic protons observed in **BzMIm-3F**, a singlet at δ_{H} 5.65, splits into two doublets at δ_{H} 5.96 and 5.34 in **1-3F**: due to coordination, the benzylic arm of the NHC ligand loses its freedom of rotation, resulting in the inequivalence of the two $-\text{NCH}_2-$ proton atoms.³¹ The resonances due to the two imidazolic $\text{NCH}=\text{CHN}$ protons were found to be significantly upshifted in **1-3F** (δ_{H} 6.87 and 6.48) compared to **BzMIm-3F** (δ_{H} 7.41 and 7.19).^{32,33} The peak due to the Cp^* proton atoms (δ_{H} 1.69) falls in the range expected for Cp^*Ir complexes reported in the literature.^{32,33} The resonances exhibited by the $^{19}\text{F}\{^1\text{H}\}$ spectrum of the deuterated chloroform solutions of **1-3F**, namely a triplet at δ_{F} - 105.75, due to the *para*-fluorine atom, and the doublet at δ_{F} - 109.87, due to the two *ortho*-fluorine atoms, are similar to those displayed by the $^{19}\text{F}\{^1\text{H}\}$ spectrum of the deuterated methanol solutions of **BzMIm-3F**.

X-ray analysis of needle-shaped, single crystals of **1-3F**, grown by diffusing *n*-pentane into CHCl_3 solutions of **1-3F** has confirmed its structure.³⁴ However, R-Factor \cong 11.05 % has prompted further, current work aimed at producing higher quality single crystals of **1-3F** in order to refine its structure to acceptable R^2 values.

Also in **1-2CH₃**, two doublets at δ_{H} 5.29 and 4.73, instead of the only singlet at δ_{H} 5.62 as in the free ligand precursor **BzMIm-2CH₃**, were observed for the two inequivalent $-\text{NCH}_2-$ methylenic protons.³¹ The rest of the resonances observed in the ^1H and $^{13}\text{C}\{^1\text{H}\}$ NMR spectra of the deuterated chloroform solutions of **1-2CH₃** are similar to those, previously discussed, of **BzMIm-2CH₃**, with the exception of that due to the coordinating carbene

32 (a) U. Hintermair, J. Campos, T.P. Brewster, L.M. Pratt, N.D. Schley, R.H. Crabtree, ACS Catal. 4 (2014) 99; (b) U. Hintermair, U. Englert, W. Leitner, Organometallics 30 (2011) 3726; (c) A.C. Marr, M. Nieuwenhuyzen, C.L. Pollock, G.C. Saunders, Organometallics 26 (2007) 2659; (d) R. Corberán, M. Sanaú, E. Peris, J. Am. Chem. Soc. 128 (2006) 3974.

33 (a) Z. Codolà, J.M.S. Cardoso, B. Royo, M. Costas, J. Lloret-Fillol, Chem. Eur. J. 19 (2013) 7203; (b) T.K. Maishal, J.-M. Basset, M. Boualleg, C. Copéret, L. Veyre, C. Thieuleux, Dalton Trans. (2009) 6956.

34 F. Lorenzini, F. Marchetti, A.C. Marr et al. (2016) unpublished results.

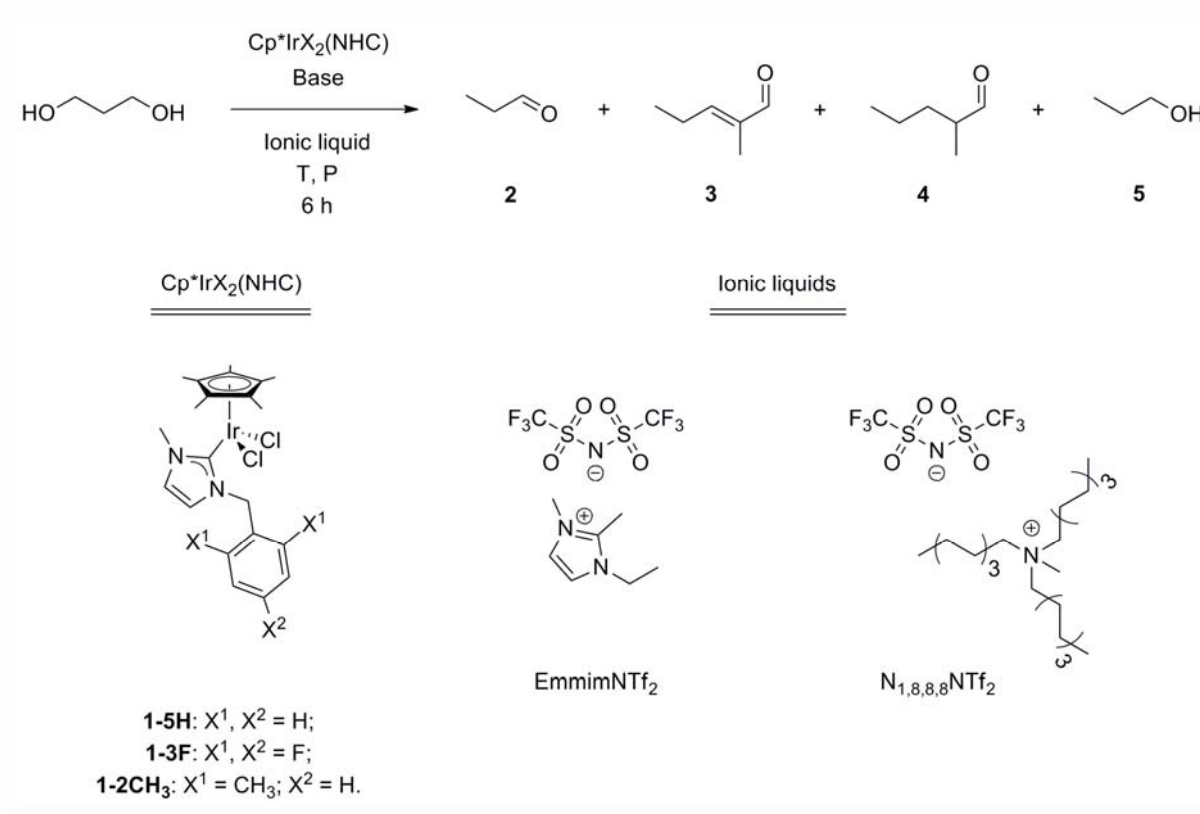
carbon atom, that is deshielded to δ_C 155.33 in **1-2CH₃**, and with the addition of the signals due to the Cp* carbon atoms at δ_C 88.80 (C₅) and 9.56 (CH₃).

HTID of 1,3-PDO: catalytic tests using catalyst precursors 1-3F and 1-2CH₃.

Complexes **1-3F** and **1-2CH₃** were then tested as catalyst precursors for HTID of 1,3-PDO in ionic liquids.

Testing catalyst precursor 1-3F.

The treatment of 1,3-PDO with **1-3F** and a base, in an ionic liquid (EmmimNTf₂ or N_{1,8,8,8}NTf₂) solution, was found to lead to a range of C3 and C6 alcohols and aldehydes (see Scheme 2): the major products observed were the C3 aldehyde propionaldehyde (**2**), and the C6 aldehydes 2-methyl-pentenal (**3**) and 2-methyl-pentanal (**4**), along with 1-propanol (**5**) as the major by-product (Scheme 2). The range of products is similar to that, recently reported by this group, observed when using **1-5H** as the catalyst precursor.¹⁴



Scheme 2. HTID of 1,3-PDO catalysed by Cp*IrX₂(NHC) complexes, in the presence of a base, in ionic liquids, at different temperatures and pressures: major reaction products; structure of the catalyst precursor complexes **1-5H**, **1-3F** and **1-2CH₃**, and of the ionic liquids EmmimNTf₂ and N_{1,8,8,8}NTf₂ tested as the solvent media.

The postulated reaction mechanism for the base-assisted HTID of 1,3-PDO catalysed by Cp*IrX₂(NHC) complexes is shown in Scheme 3. Formation of the target C3 aldehyde **2** occurs *via* the HTID of 1,3-PDO through the intermediates 3-hydroxypropionaldehyde and acrolein. Access to C6 chemistry occurs if **2** is allowed to further react after its formation: self-aldol-condensation of **2** yields, after dehydration, **3**. Hydrogenation of **3** leads to **4**.^{12,14} Both **2** and acrolein can undergo hydrogenation to the major by-product **5**. Further production of hydrogen could result from formaldehyde, formed, along with acetaldehyde, *via* the retro-aldol condensation of the hydrogen transfer intermediate 3-hydroxypropionaldehyde, and dehydrogenation of alkyl chains to olefins; spectroscopic evidence supports formation of small quantities of acetaldehyde and olefins in the reaction solutions. Decarbonylation of aldehydes, deriving from dehydrogenation of primary alcohols, to shorter alkanic and alkenic chains should also be taken into account when assessing the possible products resulting from HTID of 1,3-PDO. B. Likozar and co-workers have investigated the hydrodeoxygenation (HDO) and cracking, in the presence of heterogeneous NiMo/Al₂O₃,^{35,36,37} MoS₂,^{38,36} MoO₂,³⁸ Mo₂C,³⁸ WS₂,³⁸ Pd/Al₂O₃,³⁶ and Pd/C³⁹ catalysts, of levulinates³⁹ produced by solvolysis of lignocellulosic biomass: while secondary alcoholic groups undergo, selectively, the HDO pathway to alkanes *via* dehydration followed by hydrogenation, primary alcoholic groups tend to rather dehydrogenate to the corresponding aldehydes; the following decarbonylation produces short chain alkenes.

Taking all the above into account, specific target compounds resulting from HTID of 1,3-PDO can be obtained by tuning the reaction conditions in order to maximise selectivity towards the target and minimise by-product formation. Running the HTID of 1,3-PDO in ionic liquids under vacuum allows removal of **2** from the reaction mixture as soon as it is formed, minimising the occurrence of the side-reactions leading to **3**, **4** and **5**, and so providing crude products rich in the target C3 aldehyde **2**. Operating the reaction, instead, under pressure would drive the HTID of 1,3-PDO into a different chemical scenario: access to the C6 aldehydes chemistry would be provided, with **2** being consumed to produce **3** and **4**.⁴⁰

35 M. Grilc, B. Likozar, J. Levec, *Catal. Today* 256 (2015) 302.

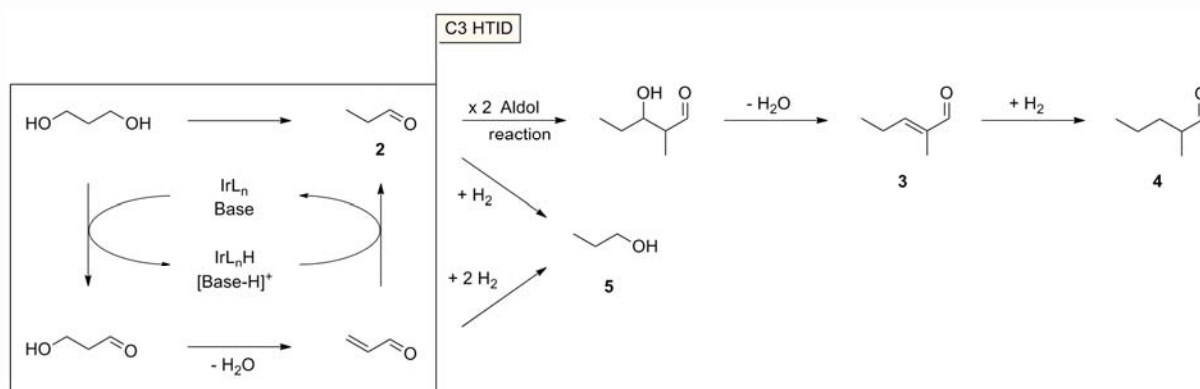
36 M. Grilc, B. Likozar, J. Levec, *Appl. Catal., B* 150-151 (2014) 275.

37 M. Grilc, B. Likozar, J. Levec, *Biomass Bioenergy* 63 (2014) 300.

38 M. Grilc, G. Veryasov, B. Likozar, A. Jesih, J. Levec, *Appl. Catal., B* 163 (2015) 467.

39 T. Yamada, H. Ono, *J. Wood Sci.* 47 (2001) 458.

40 (a) Y. Ma, F. Lorenzini, A.C. Marr (2017) unpublished results; (b) F. Lorenzini, A.C. Marr et al., conference proceedings, ISGC 2017, The International Symposium on Green Chemistry 2017, May 16-19, 2017, La Rochelle, France; (c) Y. Ma, F. Lorenzini, A.C. Marr et al., conference proceedings, 9th International Conference on Environmental Catalysis 2016, July 10-13, 2016, Newcastle, New South Wales, Australia; (d) F. Lorenzini, A.C. Marr et al., conference proceedings, CSC 2016 Conference and Exhibition, June 5-9, 2016,



Scheme 3. Postulated reaction mechanism for C3 and C6 aldehydes synthesis from base-assisted HTID of 1,3-PDO catalysed by $\text{Cp}^*\text{IrX}_2(\text{NHC})$ complexes.

The HTID of 1,3-PDO was therefore successfully driven towards the selective production of **2** by reacting 1,3-PDO in the presence of the Ir(III) complex **1-3F** ($[\text{1,3-PDO}]:[\text{Ir}] = 74.4 - 408.2$) and a base (K_2CO_3 , or KOH , or CsCO_3 ; $[\text{Base}]:[\text{1,3-PDO}] = 0.0229 - 0.0461$), in the ionic liquids EmmimNTf_2 , or $\text{N}_{1,8,8,8}\text{NTf}_2$, at temperatures varying in the range $100 - 180\text{ }^\circ\text{C}$, and at a dynamic vacuum of *ca.* 0.35 bar (see tables 1 and S1, 2 and S9, S2 and S31, S3 and S32, S4 and S33, S5 and S34, S6 and S35, S7 and S36, S10 and S37). Both ^1H NMR and GC/MS spectra of the isolated, crude product of HTID of 1,3-PDO run in the presence of complex **1-3F**, at the above conditions, show that **2** is the largely dominant species (^1H NMR: triplet at δ_{H} 9.78, $\text{C}(\text{O})\text{H}$; GC: 1.7 min). The ^1H NMR spectra also display, in the aldehydic region, the resonances due to the small or trace amount of by-products: the small intensity singlet at δ_{H} 9.38 corresponding to **3** (GC: 6.7, 9.1 min), the doublet at δ_{H} 9.60 due to very minor amounts of **4** (GC: 4.7, 8.6 min), and, at higher fields, a triplet of small intensity at δ_{H} 3.59 due to the CH_2OH protons of **5** (GC: 2.0 min).

To the best of our knowledge, the selective, homogeneous transformation of 1,3-PDO into **2** was only reported in 2016, by this group, using the non-fluorinated version of the $\text{Cp}^*\text{IrX}_2(\text{NHC})$ complex **1-3F**, namely **1-5H**, as the catalyst precursor for HTID.¹⁴

HTID yields and selectivities were observed to depend on the $\text{Cp}^*\text{IrCl}_2(\text{NHC})$ pre-catalyst loading, the nature and loading of the base, the ionic liquid used as the solvent, and the reaction temperature. The influence of each of these factors on the selectivity towards the

Halifax, NS, Canada; (e) F. Lorenzini, A.C. Marr et al., conference proceedings, UKCC 2016, Loughborough, England, UK, January 6-8, 2016; (f) F. Lorenzini, A.C. Marr et al., conference proceedings, 2nd EuGSC, 2nd EuCheMS Congress on Green and Sustainable Chemistry, Lisbon, Portugal, October 4-7, 2015.

C3 aldehyde **2**, the C6 aldehydes **3** and **4**, and the alcohol **5**, and total yields of **2-5** was then investigated (see Table 1).

Table 1. HTID of 1,3-PDO in the presence of **1-3F** and a base, in ionic liquids: total yields of **2-5**, selectivity towards **2, 3, 4**, and **5**, and TOF.

Entry	Solvent	Catalyst	[1,3-PDO]:[Ir]	Base	[Base]:[1,3-PDO]	T	% Yield (2-5) ^a	2	3	4	5	TOF ^b [s ⁻¹] (×10 ³)
1	N _{1,8,8,8} NTf ₂	1-3F	210.5	K ₂ CO ₃	0.0304	150	18	74.2	9.0	3.8	13.1	1.72
2	N _{1,8,8,8} NTf ₂	1-3F	99.5	K ₂ CO ₃	0.0305	150	50	85.4	2.9	1.4	10.2	2.29
3	N _{1,8,8,8} NTf ₂	1-3F	76.7	K ₂ CO ₃	0.0317	150	64	72.8	12.5	0.0	14.7	2.26
4	N _{1,8,8,8} NTf ₂	1-3F	408.2	K ₂ CO ₃	0.0309	120	1	30.2	2.6	0.0	67.1	0.18
5	N _{1,8,8,8} NTf ₂	1-3F	76.8	K ₂ CO ₃	0.0309	120	19	73.7	8.9	2.5	14.9	0.68
6	N _{1,8,8,8} NTf ₂	1-3F	77.0	K ₂ CO ₃	0.0303	100	1	71.8	28.2	0.0	0.0	0.05
7	N _{1,8,8,8} NTf ₂	1-3F	210.7	K ₂ CO ₃	0.0306	100	< 0.5	/	/	/	/	/
8	N _{1,8,8,8} NTf ₂	1-3F	77.7	KOH	0.0276	150	42	88.8	1.5	0.0	9.7	1.52
9	N _{1,8,8,8} NTf ₂	1-3F	211.7	KOH	0.0254	150	50	82.1	8.5	0.0	9.4	4.94
10	N _{1,8,8,8} NTf ₂	1-3F	211.1	KOH	0.0256	120	5	82.8	4.3	1.4	11.6	0.48
11	N _{1,8,8,8} NTf ₂	1-3F	76.7	KOH	0.0270	120	23	84.7	2.9	1.4	11.0	0.83
12	N _{1,8,8,8} NTf ₂	1-3F	77.2	KOH	0.0271	100	1	53.4	4.6	0.9	41.1	0.05
13	N _{1,8,8,8} NTf ₂	1-3F	210.8	KOH	0.0273	100	< 0.5	/	/	/	/	/
14	N _{1,8,8,8} NTf ₂	1-3F	208.8	CsCO ₃	0.0309	150	31	80.7	4.2	1.4	13.8	3.04
15	N _{1,8,8,8} NTf ₂	1-3F	206.2	K ₂ CO ₃	0.0309	180	39	90.8	3.1	0.0	6.1	3.76
16	EmmimNTf ₂	1-3F	211.3	K ₂ CO ₃	0.0309	180	100	87.1	3.0	0.0	9.9	9.76
17	EmmimNTf ₂	1-3F	212.4	K ₂ CO ₃	0.0311	150	70	72.7	8.8	1.2	17.3	6.86
18	EmmimNTf ₂	1-3F	212.6	K ₂ CO ₃	0.0309	120	24	72.7	8.8	6.1	12.4	2.37
19	EmmimNTf ₂	1-3F	211.4	K ₂ CO ₃	0.0303	100	7	29.4	47.2	13.4	9.9	0.65
20	EmmimNTf ₂	1-3F	399.6	K ₂ CO ₃	0.0307	150	18	49.1	16.9	2.5	31.5	3.35
21	EmmimNTf ₂	1-3F	96.6	K ₂ CO ₃	0.0309	150	81	68.4	9.4	2.3	19.8	3.62
22	EmmimNTf ₂	1-3F	403.9	K ₂ CO ₃	0.0311	120	6	49.0	18.6	9.9	22.5	1.05
23	EmmimNTf ₂	1-3F	210.9	K ₂ CO ₃	0.0310	180	41	84.1	7.2	0.0	8.7	3.98
24	EmmimNTf ₂	1-3F	77.1	K ₂ CO ₃	0.0309	180	63	84.1	7.2	0.0	8.7	2.26
25	EmmimNTf ₂	1-3F	80.3	K ₂ CO ₃	0.0309	150	85	83.6	4.3	0.0	12.1	3.17
26	EmmimNTf ₂	1-3F	76.7	K ₂ CO ₃	0.0305	120	53	73.6	6.3	7.5	12.6	1.89
27	EmmimNTf ₂	1-3F	76.7	K ₂ CO ₃	0.0312	100	20	75.1	3.9	14.0	7.0	0.72
28	EmmimNTf ₂	1-3F	77.1	KOH	0.0283	180	24	89.2	1.5	0.0	9.2	0.86
29	EmmimNTf ₂	1-3F	207.2	KOH	0.0280	180	85	86.3	3.0	0.0	10.7	8.19
30	EmmimNTf ₂	1-3F	212.8	KOH	0.0461	150	20	73.8	10.2	0.0	16.0	1.93
31	EmmimNTf ₂	1-3F	77.8	KOH	0.0283	150	79	87.6	1.5	0.0	10.9	2.83
32	EmmimNTf ₂	1-3F	102.1	KOH	0.0229	150	38	78.5	0.0	0.0	21.5	1.78
33	EmmimNTf ₂	1-3F	208.8	KOH	0.0275	150	85	88.8	1.5	0.0	9.7	8.18
34	EmmimNTf ₂	1-3F	395.6	KOH	0.0275	150	44	85.4	2.9	1.4	10.2	8.02
35	EmmimNTf ₂	1-3F	76.4	KOH	0.0272	120	33	79.6	2.7	4.0	13.6	1.18
36	EmmimNTf ₂	1-3F	207.9	KOH	0.0259	120	37	77.5	5.3	3.9	13.2	3.54
37	EmmimNTf ₂	1-3F	212.1	CsCO ₃	0.0305	150	58	86.3	3.0	0.0	10.7	5.71
38	N _{1,8,8,8} NTf ₂	No catalyst	/	K ₂ CO ₃	0.0312	150	< 0.5	/	/	/	/	/
39	EmmimNTf ₂	1-3F	213.2	No base	/	150	< 0.5	/	/	/	/	/

All operations were carried out (a) at P = 0.35 bar; (b) with reaction time: 6 h; (c) at RPM: 1000; (d) with n(1,3-PDO) ≅ 16 mmol and n(solvent) ≅ 7 mmol. ^a Crude, isolated product. ^b TOF = n(product formed) / [n(catalyst) × time].

The pre-catalyst Cp*IrX₂(NHC) complex **1-3F**, and the base, are indispensable for the HTID of 1,3-PDO to occur. 1,3-PDO remains unreacted in the absence of **1-3F** (in Table 1, see entry 38). When the HTID is carried out in the presence of **1-3F**, but in the absence of base, no reaction of 1,3-PDO is observed (in Table 1, see entry 39).

The effect of different bases, assisting the HTID of 1,3-PDO, on the total yields of **2-5** and selectivity towards **2**, **3**, **4**, and **5** was then investigated. In the range of temperatures 100 – 150 °C, K₂CO₃ and KOH allowed the highest total yields of **2-5** (85 and 89 %, respectively) and selectivities towards **2** (85 %, for both of them) as compared to CsCO₃. In general, KOH allowed a better catalytic performance than K₂CO₃ and CsCO₃. For example, when running the HTID of 1,3-PDO at 150 °C, at [1,3-PDO]:[Ir] ≅ 210.0, in EmmimNTf₂, the total yield of **2-5** was found to be 85 % in the presence of KOH (in Table 1, see entry 33), and 70 and 58 % in the presence of K₂CO₃ (in Table 1, see entry 17) and CsCO₃ (in Table 1, see entry 37), respectively. The selectivity towards **2** was high in the presence of any of the bases tested: 89, 73 and 86 % in the presence of KOH, K₂CO₃ and CsCO₃, respectively. Small, traces, or no measurable amount of the C6 aldehydes **3** (2, 9, and 3 % in the presence of KOH, K₂CO₃ and CsCO₃, respectively), and **4** (0, 1, and 0 % in the presence of KOH, K₂CO₃ and CsCO₃, respectively) were detected using any of the above bases. 10, 17, and 11 % of **5** was observed to have formed in the presence of KOH, K₂CO₃ and CsCO₃, respectively.

A similar trend was observed when running the HTID of 1,3-PDO still at 150 °C and at [1,3-PDO]:[Ir] ≅ 210.0, but in N_{1,8,8}NTf₂. High selectivities towards the C3 aldehyde **2** were observed when using KOH (82 %), K₂CO₃ (74 %), and CsCO₃ (81 %) (in Table 1, see entries 9, 1, and 14, respectively). The highest total yields of **2-5** were still observed in the presence of KOH, as compared to K₂CO₃ and CsCO₃, although they were much lower than those observed in EmmimNTf₂: 50 vs. 85 %, 18 vs. 70 %, and 31 vs. 58 %, in the presence of KOH, K₂CO₃ and CsCO₃, respectively.

The high yields and selectivity towards **2** that were achievable when using both KOH and K₂CO₃, prompted us to select K₂CO₃ as the preferable assisting base for the HTID of 1,3-PDO. Previous and current studies conducted by this group^{14,40} on the selective production of C3 and C6 aldehydes using base-assisted HTID of 1,3-PDO using Ir(III) complex Cp*IrX₂(NHC) as the catalyst precursors, have shown that yields and selectivities are affected by the base molar concentration, and have led to the conclusion that the optimal ratio [K₂CO₃]:[1,3-PDO] to be used for the selective production of **2**, with high total yields of **2-5**, is [K₂CO₃]:[1,3-PDO] ≅ 0.031. Higher and lower base concentrations would result in lower yields, and lower selectivities. We speculate that the higher base concentration may stimulate

side-reactions, including dehydrogenation, retro-aldol condensation, catalyst deactivation, and orthometallation^{32d} of the Cp*IrX₂(NHC) complex.

The effect of the two ionic liquids, as the solvent media, on the total yields of **2-5** and selectivity towards **2**, **3**, **4**, and **5** was further investigated. The better performance of the HTID of 1,3-PDO towards the selective production of **2** in EmmimNTf₂, compared to N_{1,8,8,8}NTf₂, was confirmed under further reaction conditions. For example, when running the HTID of 1,3-PDO at [1,3-PDO]:[Ir] \cong 77, using K₂CO₃, the total yields of **2-5** were found to be much higher in EmmimNTf₂ than in N_{1,8,8,8}NTf₂, at any reaction temperature (85 vs. 64 % at 150 °C - in Table 1, see entries 25 and 3, respectively; 53 vs. 19 % at 120 °C - see entries 26 and 5, respectively). However, the selectivity towards **2** remained high in both EmmimNTf₂ and N_{1,8,8,8}NTf₂, namely 84 and 73 %, respectively, at 150 °C, and 74 %, in both of them, at 120 °C. Small, traces or no measurable amount of **3** (4 and 6 %, at 150 and 120 °C, respectively, in EmmimNTf₂; 13 and 9 %, at 150 and 120 °C, respectively, in N_{1,8,8,8}NTf₂), **4** (0 and 8 %, at 150 and 120 °C, respectively, in EmmimNTf₂; 0 and 3 %, at 150 and 120 °C, respectively, in N_{1,8,8,8}NTf₂) and **5** (12 and 13 %, at 150 and 120 °C, respectively, in EmmimNTf₂; 15 % at both 150 °C and 120 °C, in N_{1,8,8,8}NTf₂) were detected in both EmmimNTf₂ and N_{1,8,8,8}NTf₂. In particular, the use of EmmimNTf₂ allowed significant conversions and selectivity towards **2** also at 100 °C, a low temperature for efficient HT reactions to occur: 20 % total yield of **2-5** was observed, with high selectivity towards **2** (75 %) (in Table 1, see entry 27). Only 1 % total yield of **2-5** was instead achieved in N_{1,8,8,8}NTf₂ at 100 °C, and, although the selectivity towards **2** was found to be high (72 %) (in Table 1, see entry 6), a high amount of the unsaturated C₆ aldehyde **3** was detected in the isolated crude product (28 %, vs. 4 % in EmmimNTf₂).

A similar trend was observed when using KOH, instead, as the assisting base. For example, when running the HTID of 1,3-PDO at [1,3-PDO]:[Ir] \cong 77, while high selectivity towards **2** was detected in both EmmimNTf₂ and N_{1,8,8,8}NTf₂ (88 and 89 % at 150 °C -in Table 1, see entries 31 and 8-, respectively, and 80 and 85 % at 120 °C -in Table 1, see entries 35 and 11-, respectively), higher total yields of **2-5** were observed in EmmimNTf₂ compared to N_{1,8,8,8}NTf₂: 79 vs. 42 % at 150 °C, and 33 vs. 23 % at 120 °C.

The different HTID performance observed in the two solvent media, EmmimNTf₂ and N_{1,8,8,8}NTf₂, must be due to some chemical influence of the ionic liquid in the reaction mechanism.⁹ Both the ionic liquids have been found to be stable throughout the HTID. The ¹H NMR spectra of the reacting mixtures show that no decomposition of the ionic liquids occurs during the course of the reaction. The triplet at δ_{H} 0.86 due to the -CH₂CH₃ methyl

protons, the singlet at 2.92 due to the -NCH₃ methylic protons, and the multiplet at δ_{H} 3.18 due to the -NCH₂- methylenic protons of N_{1,8,8,8}NTf₂ remain unchanged throughout the reaction time. The resonances due to the protons of EmmimNTf₂, namely the triplet at δ_{H} 1.51 due to the -CH₂CH₃ methylic protons, the quartet at δ_{H} 4.14 due to the -CH₂CH₃ methylenic protons, and the two doublets at δ_{H} 7.62 and 7.63 due to the two HC=CH imidazolic protons also remain unchanged.

The effect of the pre-catalyst loading on the total yields of **2-5** and selectivity towards **2**, **3**, **4**, and **5** was investigated. Increasing the pre-catalyst loading was found to enhance the catalytic performance when using K₂CO₃ as the assisting base. For example, when running the HTID of 1,3-PDO at 150 °C, at [K₂CO₃]:[1,3-PDO] \cong 0.031, in N_{1,8,8,8}NTf₂, the total yields of **2-5** were found to increase from 18, to 50, to 64 %, when increasing the pre-catalyst loading from [1,3-PDO]:[Ir] \cong 210.0, to *ca.* 100.0, to *ca.* 75.0. However, at any ratio [1,3-PDO]:[Ir], high selectivities towards **2** were observed: 74 % at [1,3-PDO]:[Ir] \cong 210.0, 85 % at [1,3-PDO]:[Ir] \cong 100.0, and 73 % at [1,3-PDO]:[Ir] \cong 75.0 (in Table 1, see entries 1-3). Selectivities towards the C6 aldehydes **3** and **4** (**3**: 3 – 13 %; **4**: 0 - 4 %) and **5** (10 – 15 %) remained low at any ratio [1,3-PDO]:[Ir]. An analogous trend was observed in EmmimNTf₂, at the same reaction conditions. High or very high selectivities towards **2** were observed at [1,3-PDO]:[Ir] \geq 210.0. Increasing the pre-catalyst loading from [1,3-PDO]:[Ir] \cong 400.0, to *ca.* 210.0, to *ca.* 100.0, to *ca.* 75.0, resulted in enhanced total yields of **2-5** from 18, to 70, to 81, to 85 % (in Table 1, see entries 20, 17, 21, and 25, respectively). In EmmimNTf₂, unlike in N_{1,8,8,8}NTf₂, the catalyst loading also affects products selectivities. The selectivity towards the C3 aldehyde **2** rises from 49 to 84 % when increasing the catalyst loading from [1,3-PDO]:[Ir] \cong 400.0, to *ca.* 75.0 (selectivity towards **2** was found to be 73 and 68 % at [1,3-PDO]:[Ir] \cong 210.0, and *ca.* 100.0, respectively). At [1,3-PDO]:[Ir] \cong 400.0, when the selectivity towards **2** is poorer, significant amount of **3** (17 %) and **5** (32 %), higher than usual, were detected in the isolated crude product.

Catalyst loading was found to have a less significant effect on the performance of **1-3F** as the catalyst precursor when running the HTID of 1,3-PDO in the presence of KOH as the assisting base. For example, when running the HTID of 1,3-PDO at 150 °C, in EmmimNTf₂, the total yield of **2-5** was found to be 85 and 79 % at [1,3-PDO]:[Ir] \cong 210.0, and *ca.* 75.0, respectively. The selectivity towards **2** was also found to be similar, and remarkably high, namely 89 % at [1,3-PDO]:[Ir] \cong 210.0, and 88 % at [1,3-PDO]:[Ir] \cong 75.0 (in Table 1, see entries 33 and 31, respectively), with no or trace amounts of C6 aldehydes **3** (2 %) and **4** (0 %), and small amounts of **5** (10 – 11 %), being formed. At the same conditions, but in

$N_{1,8,8,8}NTf_2$, the total yields of **2-5** were again found to be similar, 50 and 42 %, at [1,3-PDO]:[Ir] \cong 210.0 and 75.0, respectively, and lower than those found in EmmimNTf₂ (confirming the above trend regarding the ionic liquid effect). Also in $N_{1,8,8,8}NTf_2$, the reaction showed to be highly selective towards **2** at any ratio [1,3-PDO]:[Ir] ([1,3-PDO]:[Ir] \cong 210.0: 82 %; [1,3-PDO]:[Ir] \cong 75.0: 89 %) (in Table 1, see entries 9 and 8, respectively); only small amounts of **3**, **4**, and **5** were observed to be formed (0 – 10 %). However, when lowering the temperature to 120 °C, while still only little changes are observed with regards to both total yields of **2-5** (37 % at [1,3-PDO]:[Ir] \cong 210.0, and 33 % at [1,3-PDO]:[Ir] \cong 75.0) and selectivity towards **2** (78 % at [1,3-PDO]:[Ir] \cong 210.0, and 80 % at [1,3-PDO]:[Ir] \cong 75.0) when running the HTID of 1,3-PDO in EmmimNTf₂ (in Table 1, see entries 36 and 35, respectively), significant total yield of **2-5** was instead observed in $N_{1,8,8,8}NTf_2$ only at [1,3-PDO]:[Ir] \cong 75.0 (23 %; selectivity towards **2**: 85 %) (in Table 1, see entry 11); at lower catalyst loading ([1,3-PDO]:[Ir] \cong 210.0), only 5 % total yield of **2-5** (selectivity towards **2**: 83 %) was obtained (in Table 1, see entry 10).

The effect of the temperature on the reaction yields and selectivity was then investigated. Significant production of **2** at 100 °C was observed only in EmmimNTf₂, at [1,3-PDO]:[Ir] \cong 75.0, using K₂CO₃ as the assisting base: 20 % total yield of **2-5** was obtained, with 75 % selectivity towards **2** (in Table 1, see entry 27). Little traces of, or no crude was obtained when running the HTID of 1,3-PDO at 100 °C, at any other reaction conditions (in Table 1, see entries 6, 7, 12, 13, and 19). In general, increasing the temperature to 120 °C and 150 °C resulted in significant enhancements in the reaction yield, reaching maximum total yields of **2-5** of 85 % at 150 °C (in Table 1, see entries 25 and 33). Small rises in selectivity towards **2** were observed correspondingly. For example, when running the HTID of 1,3-PDO in $N_{1,8,8,8}NTf_2$, at [1,3-PDO]:[Ir] \cong 75.0, and [K₂CO₃]:[1,3-PDO] \cong 0.031, the total yield of **2-5** rose from 1 to 19 to 64 % when increasing the temperature from 100 °C, to 120 °C, to 150 °C, respectively. Correspondingly, the selectivity towards **2** remained high and changed little (72, 74, and 73 %, respectively) (in Table 1, see entries 6, 5 and 3, respectively). The total yield of **2-5** rose from 20 to 53, to 85 % when the temperature was increased from 100 °C, to 120 °C, to 150 °C, respectively, running the HTID of 1,3-PDO under the same conditions, but in EmmimNTf₂, and the selectivity towards **2** was little affected (75, 74, 84 %, respectively) (in Table 1, see entries 27, 26 and 25, respectively).

Increasing the temperature to 180 °C allowed quantitative total yields of **2-5**, with high selectivity towards the C3 aldehyde (87 %), when running the HTID of 1,3-PDO in EmmimNTf₂, at [1,3-PDO]:[Ir] \cong 210.0, and [K₂CO₃]:[1,3-PDO] \cong 0.031 (in Table 1, see

entry 16). At other reaction conditions, increasing the temperature from 150 °C to 180 °C resulted in little or detrimental effect on the total yields of **2-5**.

The HTID of 1,3-PDO to **2** in the presence of **1-3F** was proven to be homogeneous *via* mercury poisoning experiments:^{32a} the catalytic activity of **1-3F** remained essentially unchanged in the presence of mercury (see Table 2).

Furthermore, the catalytic system is not sensitive to air and tolerated the presence of water. Highly selective production of **2** (86 %) was observed when running the HTID of 1,3-PDO in EmmimNTf₂, in the presence of **1-3F** and K₂CO₃, and a significant amount of water.

Table 2. HTID of 1,3-PDO in the presence of **1-3F** and K₂CO₃, and in the presence (entry 1) or absence (entry 2) of mercury,^a in EmmimNTf₂: total yields of **2-5**, selectivity towards **2**, **3**, **4**, and **5**, and TOF. (Entries 1 and 2 correspond to entry 1 in tables S9, S19, S29, and entry 25 in tables S1, S11, S21, respectively.)

Entry	Solvent	Catalyst	[1,3-PDO]:[Ir]	Base	[Base]:[1,3-PDO]	T	% Yield (2-5) ^b	2	3	4	5	TOF ^c [s ⁻¹] (×10 ³)
1	EmmimNTf ₂	1-3F	77.7	K ₂ CO ₃	0.0308	150	86	73.0	8.8	0.0	18.1	3.08
2	EmmimNTf ₂	1-3F	80.3	K ₂ CO ₃	0.0309	150	85	83.6	4.3	0.0	12.1	3.17

All operations were carried out (a) at P = 0.35 bar; (b) with reaction time: 6 h; (c) at RPM: 1000; (d) with n(1,3-PDO) ≅ 16 mmol and n(solvent) ≅ 7 mmol. ^a Amount of mercury added: 3 drops. ^b Crude, isolated product. ^c TOF = n(product formed) / [n(catalyst) × time].

Recycling catalyst precursor 1-3F.

The evidence collected screening the effect of the reaction conditions on the yields of, and selectivity towards, the C3 aldehyde **2** prompted us to investigate the recyclability of the **1-3F** catalyst precursor running the HTID of 1,3-PDO in EmmimNTf₂, using K₂CO₃ as the assisting base, at [K₂CO₃]:[1,3-PDO] \cong 0.031, at both [1,3-PDO]:[Ir] \cong 210.0 and *ca.* 75.0, and at both 120 °C and 150 °C.

1-3F was found to be a highly recyclable catalyst precursor. The catalytic system generated by **1-3F** was found to be recyclable for at least 10 catalytic runs at both 120 °C and 150 °C, at catalyst loading [1,3-PDO]:[Ir] \cong 75.0. Over the 10 recycling runs, no significant loss of activity or selectivity towards **2** was observed. Figure 1 shows duplicates⁴¹ of the selectivity towards **2**, **3**, **4**, and **5**, varying little, over the 10 recycling runs, as observed when recycling **1-3F**, at [1,3-PDO]:[Ir] \cong 75.0, in EmmimNTf₂, in the presence of K₂CO₃, at 150 °C. In Figure 2, triplicates⁴² of the almost identical selectivity towards **2**, **3**, **4**, and **5**, and the total yield of **2-5**, observed when recycling **1-3F** at the same conditions, for the first five recycling runs, are represented. At 150 °C, the selectivity towards **2** remained almost unchanged (for example: 1st catalytic run: 78 %; 10th catalytic run: 79 %) (See Figure S2, and Table S32, and also figures S1 and S3, and tables S31 and S33), while the percentage total yield of **2-5** was 85 % after the 1st catalytic run, and 70 % after the 10th catalytic run, varying overall within the range 61 – 99 %.

41 ‘Duplicates’: yield and selectivity average numbers out of two experiments.

42 ‘Triplicates’: yield and selectivity average numbers out of three experiments.

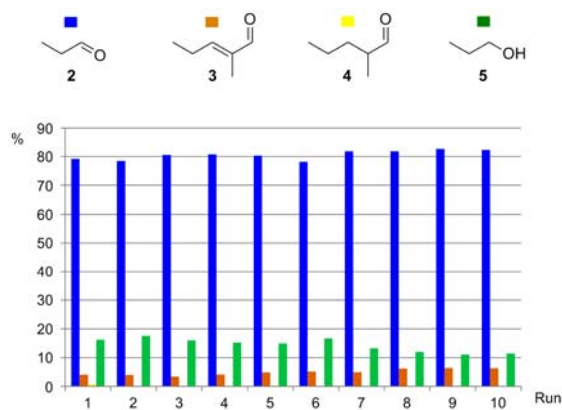


Figure 1. Recycling **1-3F** as catalyst precursor towards HTID of 1,3-PDO ([1,3-PDO]:[Ir] \cong 75.0) in EmmimNTf₂, in the presence of K₂CO₃, at 150 °C and 0.35 bar: selectivity towards **2**, **3**, **4**, and **5** (duplicates).

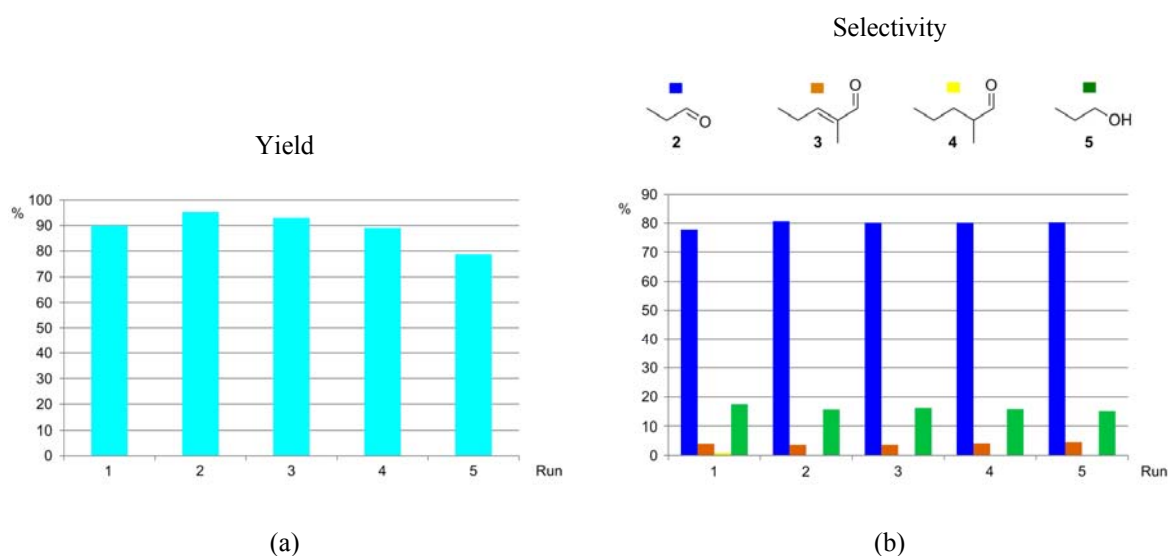


Figure 2. Recycling **1-3F** as catalyst precursor towards HTID of 1,3-PDO ([1,3-PDO]:[Ir] \cong 75.0) in EmmimNTf₂, in the presence of K₂CO₃, at 150 °C and 0.35 bar: (a) total yield of **2-5** (triplicates); (b) selectivity towards **2**, **3**, **4**, and **5** (triplicates).

No significant loss of activity or selectivity towards **2** was observed over 10 recycling runs at 120 °C. Figure 3 shows duplicates, over the first five recycling runs, of the selectivity towards **2**, **3**, **4**, and **5**, and total yields of **2-5**, varying little, as observed when recycling **1-3F**, at [1,3-PDO]:[Ir] \cong 75.0, in EmmimNTf₂, in the presence of K₂CO₃, at 120 °C. Over the 10 recycling runs, the total yield of **2-5** was 58 % after the 1st catalytic run, and 53 % after the 10th catalytic run, the percentage total yield of **2-5** varying in the range 53 – 71 % (See Figure S4, and Table S34); the selectivity towards **2** was found to be 82 % in the 1st catalytic run, and 73 % in the 10th catalytic run, varying in the range 70 – 86 %.

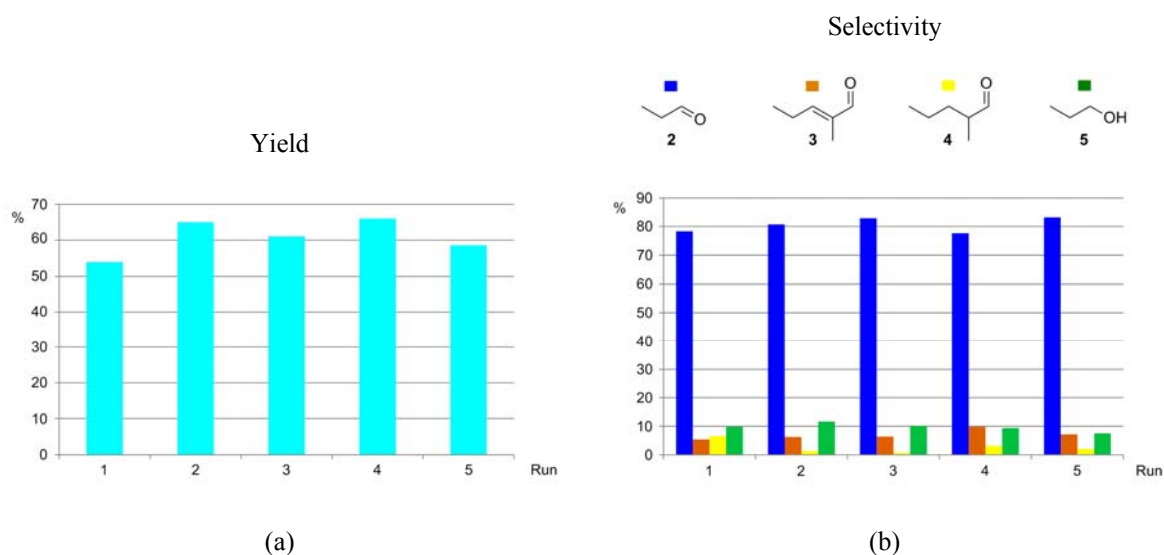


Figure 3. Recycling **1-3F** as catalyst precursor towards HTID of 1,3-PDO ($[1,3\text{-PDO}]:[\text{Ir}] \cong 75.0$) in EmmimNTf_2 , in the presence of K_2CO_3 , at $120\text{ }^\circ\text{C}$ and 0.35 bar : (a) total yield of **2-5** (duplicates); (b) selectivity towards **2, 3, 4**, and **5** (duplicates).

The catalyst precursor **1-3F** was also found to be recyclable at $[1,3\text{-PDO}]:[\text{Ir}] \cong 210.0$, when running the HTID of 1,3-PDO in EmmimNTf_2 , at $[\text{K}_2\text{CO}_3]:[1,3\text{-PDO}] \cong 0.031$, and at $150\text{ }^\circ\text{C}$. The catalyst was found to be recyclable for at least 5 catalytic runs. Also in this case, no significant loss of selectivity towards **2** or activity was observed: the selectivity towards **2** varied in the range $82 - 85\%$, while the percentage total yield of **2-5** was found to be 78% in the 1st catalytic run and 76% in 5th catalytic run, varying in the range $68 - 83\%$ (See Figure S6, and Table S36).

Testing catalyst precursor **1-2CH₃**.

The HTID of 1,3-PDO was then attempted by reacting 1,3-PDO in the presence of the Ir(III) complex **1-2CH₃** and K_2CO_3 , at $[\text{K}_2\text{CO}_3]:[1,3\text{-PDO}] \cong 0.031$, at $[1,3\text{-PDO}]:[\text{Ir}] = 49.1$ and 99.1 , at temperatures $150\text{ }^\circ\text{C}$ and $120\text{ }^\circ\text{C}$, respectively, in EmmimNTf_2 , and at a dynamic vacuum of *ca.* 0.35 bar . No product formation was observed when testing **1-2CH₃** at $[1,3\text{-PDO}]:[\text{Ir}] = 99.1$ and $120\text{ }^\circ\text{C}$, while the reaction of 1,3-PDO in the presence of **1-2CH₃**, at $[1,3\text{-PDO}]:[\text{Ir}] = 49.1$, at $150\text{ }^\circ\text{C}$, produced total yields of **2-5** $\leq 0.01\%$ (see Table 3). In addition, only trace amounts of product were formed in $\text{N}_{1,8,8,8}\text{NTf}_2$: testing the activity of **1-2CH₃** at $[1,3\text{-PDO}]:[\text{Ir}] = 49.0$, at $150\text{ }^\circ\text{C}$, led to *ca.* 0.5% total yield of **2-5**.

Replacement of H or F atoms (as in the HTID-active catalyst precursors **1-5H** and **1-3F**) bound to the *ortho*-C atoms of the benzyl arm of the carbene ligand with CH_3 , has

resulted in the inhibition of the catalytic activity of complexes $\text{Cp}^*\text{IrCl}_2(\text{NHC})$ towards HTID of 1,3-PDO. The origins of this effect could be steric or electronic as the methyl grouping is the bulkiest and most electron donating group attempted. However the observation may have more profound meaning, as for C-H and C-F orthometallation is feasible, but the methyl group is unlikely to react with the metal centre. This, coupled to the remarkable activity and selectivity achieved using **1-3F** as the catalyst precursor has prompted further, current work in this group aimed at exploring fluorine substitution in the benzyl arm of the carbene ligand of $\text{Cp}^*\text{IrCl}_2(\text{NHC})$ complexes for HTID of 1,3-PDO. The beneficial or detrimental contribution of cyclometallation to HTID is being investigated.²⁹ The possibly crucial role played in cyclometallation reactions of fluorinated $\text{Cp}^*\text{IrCl}_2(\text{NHC})$ complexes, occurring *via* regiospecific carbon—fluorine bond activation, by silver particles generated in the synthesis of the Ir(NHC) complexes by transmetalation of imidazolylidenes from the corresponding silver carbene derivative to $[\text{Cp}^*\text{IrCl}_2]_2$, is being looked into.^{29a} Furthermore, the lack of activity of complex **1-2CH₃** in HTID of 1,3-PDO prevented from any further investigation on the effect of alkyl substitution in the benzyl arm of the Ir(III) complexes carbene ligand; however, the electronic and steric effects of *N*-alkyl substitution on the carbene ligand of catalyst precursors $\text{Cp}^*\text{IrCl}_2(\text{NHC})$ on HTID of 1,3-PDO for the production of value-added target chemicals is currently being investigated.⁴³ Current work is also aimed at exploiting the catalytic activity of precursors $\text{Cp}^*\text{IrCl}_2(\text{NHC})$ to drive the HTID of 1,3-PDO away from the C3 aldehyde **2** and towards the selective production of other value-added, longer chain, aldehydes.⁴⁰ The postulated reaction mechanism for the base-assisted HTID of 1,3-PDO catalysed by $\text{Cp}^*\text{IrX}_2(\text{NHC})$ complexes, coupled with self-aldol condensation of the HTID product **2**, discussed above, illustrates that C6 aldehydes chemistry can be accessed if **2** is allowed, or encouraged to further react after its formation. That can be achieved for example by running the HTID under pressure: **3**, a valuable chemical, commercially important because of its industrial applications, including in the food, pharmaceutical, cosmetic, and plasticizer fields,^{44,45,46} would be yielded *via* self-aldol-condensation of **2**, after dehydration. Current work by the authors is focused on the selective production of the valuable C6 aldehyde **3** by running the HTID of 1,3-PDO under pressure.⁴⁰

Conclusions.

43 H. Iqbal, F. Lorenzini, A.C. Marr et al. (2016) unpublished results.

44 T. Aida, T. Nagasawa, Y. Yamazaki, *WO Pat.* 065851, 2008.

45 S. Tanaka, K. Fukuda, T. Asada, *WO Pat.* 029033, 2004.

46 A.D. Godwin, R.H. Schlosberg, F. Hershkowitz, M.G. Matturro, G. Kiss, K.C. Nadler, P.L. Buess, R.C. Miller, P.W. Allen, H.W. Deckman, R. Caers, E.J. Mozeleski, R.P. Reynolds, (2001) *U.S. Patent No. 6,307,093*. Washington, DC: U.S. Patent and Trademark Office.

We have shown that the fluorinated Cp*IrCl₂(NHC) complex **1-3F** is a highly recyclable catalyst precursor for the efficient, selective production of **2** *via* HTID of 1,3-PDO in ionic liquids, under air. In comparison the related complex **1-2CH₃** has very poor catalytic activity. The use of **1-3F** in ionic liquid enables HTID to proceed under controlled, reduced pressure: that facilitates product isolation and allows high selectivity, with minimal waste. In addition, HTID of 1,3-PDO to **2** in ionic liquids is successful also when a significant volume of water is involved in the reaction. A crucial role played in HTID by the *ortho*-grouping of the carbene ligand benzyl arm of Cp*IrCl₂(NHC) complexes is suggested by the inhibition of the catalytic activity observed when removing any H and F atoms bound to the *ortho*-C atoms. The successful synthesis and isolation of a value-added chemical from the ionic liquid solutions of 1,3-PDO, representing the ionic liquid solutions extracting the diol from the aqueous glycerol fermentation broths,⁴⁷ demonstrates the valorisation of waste to chemicals. Combining bio-catalytic treatment of waste glycerol with Cp*IrX₂(NHC) - catalysed HTID of 1,3-PDO in ionic liquids has the ultimate potential to allow production of valuable chemicals, which can be simply isolated, directly from a renewable sources.

47 X.-h. Liu, M. Rebroš, I. Dolejš, A.C. Marr, ACS Sustainable Chem. Eng. DOI: 10.1021/acssuschemeng.7b01934.

Table 3. HTID of 1,3-PDO in the presence of **1-2CH₃** and K₂CO₃, in EmmimNTf₂: total yields of **2-5**, selectivity towards **2, 3, 4**, and **5**, and TOF. (Entries 1- 2 correspond to those in tables S8, S18, S28.)

Entry	Solvent	Catalyst	[1,3-PDO]:[Ir]	Base	[Base]:[1,3-PDO]	T	% Yield (2-5) ^a	2	3	4	5	TOF ^b [s ⁻¹] (×10 ³)
1	EmmimNTf ₂	1-2CH₃	49.1	K ₂ CO ₃	0.0308	150	≤ 3	1.6	0.6	0.1	97.8	0.07
2	EmmimNTf ₂	1-2CH₃	99.1	K ₂ CO ₃	0.0300	120	< 0.5	/	/	/	/	/

All operations were carried out (a) at P = 0.35 bar; (b) with reaction time: 6 h; (c) at RPM: 1000; (d) with n(1,3-PDO) ≅ 16 mmol and n(solvent) ≅ 7 mmol. ^a Crude, isolated product. ^b TOF = n(product formed) / [n(catalyst) × time].

Acknowledgements

This work was supported by GRAIL (Grant agreement no: 613667), project co-financed by the European Commission under the 7th Framework Programme. The assistance provided by Queen's University Ionic Liquid Laboratories (QUILL), and the analytical chemistry service (ASEP) and glassblowing service at Queen's University Belfast, is acknowledged.